Pergamon

Geochimica et Cosmochimica Acta, Vol. 64, No. 12, pp. 2133–2154, 2000

0016-7037/00 $20.00 + .00

PII S0016-7037(00)00355-0

Chronology and petrology of silicates from IIE iron meteorites: Evidence of a complex parent body evolution

DONALD D. BOGARD,[1,*] DANIEL H. GARRISON,[2] and TIMOTHY J. MCCOY[1,3]

[1]Planetary Sciences, SN2, NASA Johnson Space Center, Houston, TX 77058, USA
[2]Lockheed–Martin Engineering and Johnson Space Center, Houston, TX 77058, USA
[3]Department of Mineral Sciences, National Museum of Natural History, Smithsonian Institution, Washington, DC 20560-0119, USA

(*Received September* 9, 1999; *accepted in revised form January* 25, 2000)

Abstract—IIE iron meteorites contain silicate inclusions the characteristics of which suggest a parent body similar to that of H-chondrites. However, these silicates show a wide range of alteration, ranging from Netschaëvo and Techado, the inclusions of which are little altered, to highly differentiated silicates like those in Kodaikanal, Weekeroo Station, and Colomera, which have lost metal and sulfur and are enriched in feldspar. We find these inclusions to show varying degrees of shock alteration. We made ^{39}Ar–^{40}Ar age determinations of Watson, Techado, Miles, Colomera, and Sombrerete. Watson has an Ar–Ar age of 3.677 ± 0.007 Gyr, similar to previously reported ages for Kodaikanal and Netschaëvo. We suggest that the various determined radiometric ages of these three meteorites were probably reset by a common impact event. The space exposure ages for these three meteorites are also similar to each other and are considerably younger than exposure ages of other IIEs. ^{39}Ar–^{40}Ar ages inferred for the other four meteorites analyzed are considerably older than Watson and are: Techado = 4.49 ± 0.01 Gyr, Miles = 4.405 ± 0.012 Gyr, Colomera = 4.470 ± 0.010 Gyr, and Sombrerete = 4.541 ± 0.0012 Gyr. These ages are in fair agreement with previously reported Rb–Sr isochron ages for Colomera and Weekeroo Station. Although several mechanisms to form IIE meteorites have been suggested, it is not obvious that a single mechanism could produce a suite of meteorites with very different degrees of silicate differentiation and with isotopic ages that differ by >0.8 Gyr. We suggest that those IIEs with older isotopic ages are a product of partial melting and differentiation within the parent body, followed by mixing of silicate and metal while both were relatively hot. Netschaëvo and Watson may have formed by this same process or by impact mixing ~4.5 Gyr ago, but their isotopic ages may have been subsequently reset by shock heating. Kodaikanal apparently is required to have formed more recently, in which case impact melting and differentiation seems the only viable process. We see no compelling reasons to believe that IIE silicate and metal derived from different parent bodies or that the parent body of IIEs was the same as that of H-chondrites. *Copyright © 2000 Elsevier Science Ltd*

1. INTRODUCTION

The diversity among meteorites reveals that some asteroidal parent bodies apparently never were heated sufficiently to cause significant melting and differentiation (e.g., the chondrites), whereas other parent bodies were appreciably melted and differentiated to the point that surface basalt flows (e.g., eucrites) and metal cores (e.g., some iron meteorites) were formed. Still other meteorites suggest parent bodies where the degree of melting and differentiation fell in between these two extremes. On these bodies sufficient melting occurred so as to produce separation of silicate and metal and even some differentiation of silicate, but surface basalt flows and metal cores may not have been produced. Examples of these types of meteorites are the acapulcoites–lodranites and the winonaites–IAB irons, where each pair is thought to represent a single parent body. Acapulcoites–lodranites represent originally chondritic-like material heated sufficiently to differentiate and lose metal, and in the case of lodranites, also to lose a feldspar-rich, low-melting differentiate (Mittlefehldt et al., 1996; McCoy et al., 1997). Winonaites also are thought to have been derived from chondritic-like material by removal of metal (Benedix et al., 1998). In contrast, IAB irons are mostly metal, but are thought to derive from the same parent as winonaites.

The IIE irons are another group of silicate-bearing iron meteorites. They define coherent trends on element–element plots of Ni vs. Ga, Ge, Co, Cu, As, Au, W, and Ir (Wasson and Wang, 1986). Some of these trends can be readily explained by fractional crystallization of a large metallic body and might form during crystallization of a single core. Other element–element trends in IIEs are not easily explained by such a mechanism and are more similar to those in IAB irons. Wasson and Wang (1986) argue that these trends reflect formation of the metallic host by impact melting of the near-surface layer of an asteroid. The IIE irons also display a wide range of silicate inclusion types—from angular, chondrule-bearing inclusions to small globular, strongly differentiated, feldspar-rich inclusions. An unusual characteristic of IIE meteorites is that some show relatively old isotopic formation ages of ~4.5 Gyr, whereas a few indicate ages that are younger by ~0.8 Gyr (Burnett and Wasserburg, 1967a; Niemeyer, 1980; Olsen et al., 1994). Ages significantly younger than ~4.5 Gyr are seen in some other meteorite types and are commonly ascribed to resetting by large impact events (Bogard, 1995). By analogy to the IAB irons (which all have ages of ~4.5 Gyr, as far as is known) we might surmise that the IIE metal–silicate assemblage formed by igneous processes within the parent body. On the other hand,

* Author to whom correspondence should be addressed (Donald.D.Bogard@jsc.nasa.gov).

the young isotopic ages might imply formation by impact mixing at a much later time. Previous workers have invoked both internal parent body metamorphism and impact melting to explain the formation of differentiated silicates and metal–silicate mixing in the IIE irons (Mittlefehldt et al., 1998 and references therein).

Only a limited amount of data on isotopic chronology has been available for IIE meteorites. Thus, we initiated an investigation to determine the ^{39}Ar–^{40}Ar ages of silicate from four IIE meteorites (Watson, Techado, Miles, Colomera) and the ungrouped but closely related silicate-bearing iron Sombrerete. When we began our study, no precise isotopic ages existed for four of these meteorites. The ^{39}Ar–^{40}Ar technique is particularly sensitive to resetting by only moderate heating events. In addition, we measured noble gases in four of these meteorites to better estimate space exposure ages. We also made additional petrological studies of silicate in several IIE meteorites, with particular emphasis on shock features.

2. SAMPLES AND TECHNIQUES

Eight silicate-bearing iron meteorites have been classified as IIE or IIE–An on the basis of their metal compositions: Weekeroo Station, Colomera, Elga, Netschaëvo, Kodaikanal, Techado, Miles, and Watson (Wasson et al., 1986; Olsen et al., 1994). These meteorites also share a common oxygen isotopic signature, with $\Delta^{17}O$ of 0.59 ± 0.07 for all 8 (Clayton and Mayeda, 1996). Several other meteorites, which are ungrouped on the basis of their metal composition or for which the metal composition is unknown, have also been suggested to have close ties to group IIE. These include Guin (Rubin et al., 1985), Sombrerete (Prinz et al., 1983), and Yamato 791093 (Ikeda et al., 1997a). Sombrerete contains globular silicate inclusions and is similar to IIEs in many respects. Its inclusions consist of orthopyroxene, phosphate, plagioclase, SiO_2, and feldspathic glass, similar to inclusions in Weekeroo Station and Miles. However, Malvin et al. (1984) found that the Ge concentration of the metallic host and oxygen isotopic composition of Sombrerete silicate preclude grouping Sombrerete with the IIE irons. It seems most likely that Sombrerete formed in a manner analogous to those "old" IIEs with globular inclusions, but on a separate parent body.

For this petrologic study, we focused on the main group IIE irons, conducting examinations of Miles (UH 261), Techado (UNM 1054; the same section studied by Casanova et al., 1995), Weekeroo Station (USNM 835), Netschaëvo (USNM 494-3, 1096), Colomera (USNM 3396-4), Kodaikanal (USNM 2858), and Watson (UH 260). No sample of Elga was available for our study. We briefly examined PTS,51-2 of Yamato 791093 at the National Institute of Polar Research. Polished thin section and polished sections of meteorites were examined in transmitted and reflected light. Imaging, qualitative, and quantitative analyses of selected phases in silicate-bearing IIE irons were conducted by using the SX-100 electron microprobe at Johnson Space Center, Houston, Texas. Modal analyses of 400 to 1500 point were conducted on Techado and Miles.

We neutron irradiated silicate samples of Watson, Miles, Techado, Colomera (feldspar), and Sombrerete (USNM 5870) for ^{39}Ar–^{40}Ar analysis. The Miles sample was from the same silicate clast for which the petrographic description was made. The Watson sample was received from J. Schwade and is from the same large silicate inclusion studied by Olsen et al. (1994). The Colomera feldspar separate was received from G. Wasserburg and is the same material studied by Wasserburg et al. (1968) and Sanz et al. (1970). The Techado sample analyzed was received courtesy of A. Brearley (Institute of Meteoritics). It consisted of several small pieces of intergrown silicate, metal, and metal oxide from which we were able to extract only 10 mg of silicate for Ar–Ar analysis. This Techado sample is not the same inclusion studied by Casanova et al. (1995). The Sombrerete sample received was mostly metal with thin, bead-like strings of silicate. The metal was dissolved in cold, 1 N nitric acid for 3 days. This process left several white and gray inclusions a few mm in diameter. A single white inclusion weighing 13 mg was used for Ar–Ar dating and a separate inclusion for cosmogenic studies.

The five meteorite samples Ar–Ar dated, along with samples of the NL-25 hornblende age monitor, were neutron irradiated in four separate irradiations. Argon was released by stepwise degassing in a high vacuum furnace and its isotopic composition was measured on a Nuclide mass spectrometer. Argon isotopic data for each sample are given in Appendix 1. We also analyzed noble gas concentrations in unirradiated silicate samples of Netschaëvo (USNM 2957), Miles, Sombrerete, and Colomera (feldspar) for the purpose of comparing space exposure ages. Noble gases were released from these samples in two temperature steps and analyzed on a VG-3600 mass spectrometer that has not been exposed to irradiated samples. Additional details of the techniques are given in Garrison et al. (1992) and Garrison and Bogard (1998).

To interpret Ar–Ar age spectra, we use changes in the K/Ca ratio, the rate of release of different Ar isotopes as a function of temperature, and similarity among Ar–Ar ages for individual extractions to define sample phases showing similar Ar release characteristics. We calculate the average Ar–Ar age across a temperature range by weighing the age for each extraction according to the relative amount of Ar released. Each such "plateau" age has several sources of analytical uncertainty. Uncertainties in Ar data include errors in measuring isotopic ratios and uncertainties in corrections applied for system blanks and reactor-produced interferences. For the measurement uncertainty we adopt one standard deviation from the mean of ~15 individual measurements of the Ar isotopic composition. Uncertainties in applied blanks and reactor corrections are estimated from the reproducibility of multiple measurements of these parameters. We derive the overall analytical error in the $^{40}Ar/^{39}Ar$ ratio of individual extractions by taking the square root of the sum of the squares of all these individual uncertainties. A totally separate uncertainty in the Ar–Ar age derives from uncertainty in the neutron irradiation constant, J, which we estimate from measurements of several NL-25 hornblende age monitors interspersed among the samples during irradiation (Bogard et al., 1995). The analytical errors in measuring the Ar isotopic composition of these hornblendes are usually small. Another uncertainty in J comes from small geometric gradients in neutron fluence revealed by variations in $^{40}Ar/^{39}Ar$ among the hornblendes. The uncertainty in J for a sample of unknown age is estimated from its known location within the quartz vial relative to locations of the hornblendes. The value of J and its uncertainty for each meteorite sample is reported in Appendix 1.

The equation for calculating an ^{39}Ar–^{40}Ar age is $T = 1/\lambda * \ln[R * J + 1]$, where λ is the ^{40}K decay constant, R is the corrected $^{40}Ar/^{39}Ar$ ratio, and J is the irradiation constant. For each extraction temperature we calculate an uncertainty in the age considering only the uncertainty in the $^{40}Ar/^{39}Ar$ ratio. In deciding which individual extractions show similar Ar–Ar ages (i.e., an age "plateau"), only the age uncertainty contributed by $^{40}Ar/^{39}Ar$, and not that contributed by J should be considered. This is the age uncertainty given in Appendix 1 and shown in the Ar–Ar age spectra presented here. Note that most tabulated Ar–Ar ages for individual extractions previously reported from JSC have listed uncertainties compounded from both uncertainties in $^{40}Ar/^{39}Ar$ and J.

It is often the case that the greater uncertainty in deriving an overall ^{39}Ar–^{40}Ar degassing age is determined by variations among individual ages for specific extractions that one elects to include in the "plateau" age and by the uncertainty in irradiation constant J, and not by the analytical uncertainties associated with Ar isotopic measurements. To obtain the uncertainty in a calculated Ar–Ar "plateau" age, we first calculate the 1σ uncertainty in deviations of individual extraction ages from the mean (plateau) age. Next, we use partial derivatives of the age equation to combine this 1σ uncertainty in the mean age with the estimated uncertainty in the age created by the uncertainty in J (Bevington, 1969). In these calculations of error, we do not weigh individual extraction ages by the respective analytical uncertainties in $^{40}Ar/^{39}Ar$, as is sometimes done in reporting isochron ages for other isotopic chronometers. We have three reasons for not doing so. First, the Ar–Ar age uncertainties for individual extractions are usually similar. Second, uncertainties in individual ages are often smaller than the variations among individual Ar–Ar ages, a situation that is often different from other chronometer data. Third, we find that weighing of individual ages according to their $^{40}Ar/^{39}Ar$ uncertainties often gives a much lower

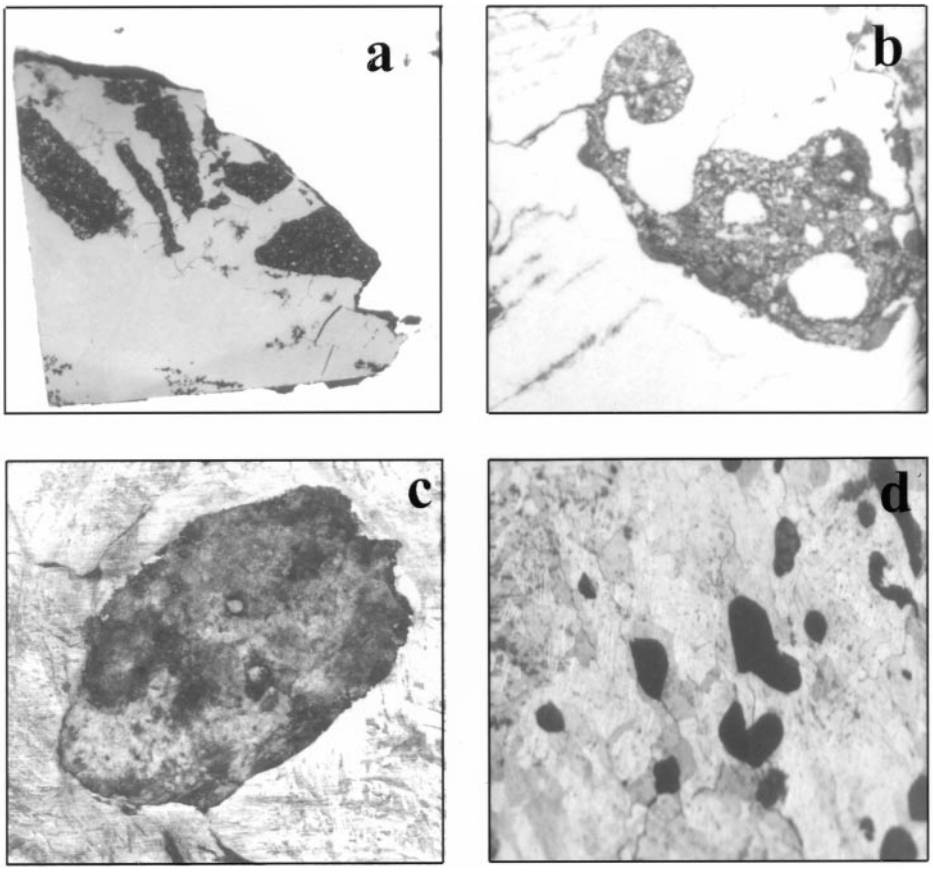

Fig. 1. Silicate inclusions in IIE iron meteorites. (a) Angular-silicate inclusions in Netschaëvo are chondrule-bearing and undifferentiated. Inclusion is 3 cm long at base. (b) A single silicate inclusion in Techado is undifferentiated, but the shape is suggestive of softening and stretching. Inclusion is 13 mm in maximum dimension. (c) The irregular inclusions in Watson are depleted in Fe, Ni metal, and troilite. Inclusion is 25 mm in length. (d) Globular, gabbroic inclusions such as these in Colomera are also found in Miles, Weekeroo Station, Kodaikanal, and Elga. Width of field of view is 25 mm.

uncertainty for the mean age, compared to the uncertainty of an unweighed mean age. This overall method of determining the error in an Ar–Ar degassing age involves diverse parameters with individual uncertainties obtained in different ways, and cannot be simply expressed as 1σ or 2σ.

The uncertainty in an ^{39}Ar–^{40}Ar age as calculated above suffice when comparing Ar-Ar ages of different samples obtained at JSC. When comparing Ar-Ar ages determined at JSC with Ar–Ar ages determined at other laboratories by using different age monitors, one should also consider uncertainties in the absolute ages of the various age monitors. We estimate the age uncertainty of hornblende NL-25 to be less than $\pm 0.5\%$ (Bogard et al., 1995). Errors given for most Ar–Ar ages in the literature do not include uncertainties in the absolute monitor ages. In addition to monitor age uncertainties, uncertainties in various decay constants (McCoy et al., 1997) also must be considered when making comparisons between Ar–Ar ages and ages derived by using other isotopic chronometers such as Rb–Sr, Sm–Nd, etc. The magnitudes of possible biases among different chronometers are not well defined. Thus, some caution should be taken in comparing radiometric ages of a common sample obtained with different chronometers.

Table 1. Modal compositions (vol.%) of silicate inclusions in IIE irons, excluding Fe,Ni metal and FeS.

	Netschaëvo	Techado	Watson	Miles	Weekeroo Station	Colomera	Kodaikanal	Elga
Olivine	26	81*	57	0	0	0	0	0
Orthopyroxene	52		23	23	24	~3	~3	~3
Clinopyroxene	5	0	5	33	16	~28	21	~28
Plag-Trid-Glass	14	19	12	43	59	67	73	68
Phosphate	2	n.d.	1	0.3	~1	~1	~1	~1
Yagite	—	—	—	—	—	~3	—	—

Sources of data: Netschaëvo, Olsen and Jarosewich (1971); Techado and Miles, this work; Watson, Prinz et al. (1994); Weekeroo Station, Colomera, Kodaikanal and Elga, Prinz et al. (1983).

* Includes both olivine and orthopyroxene.

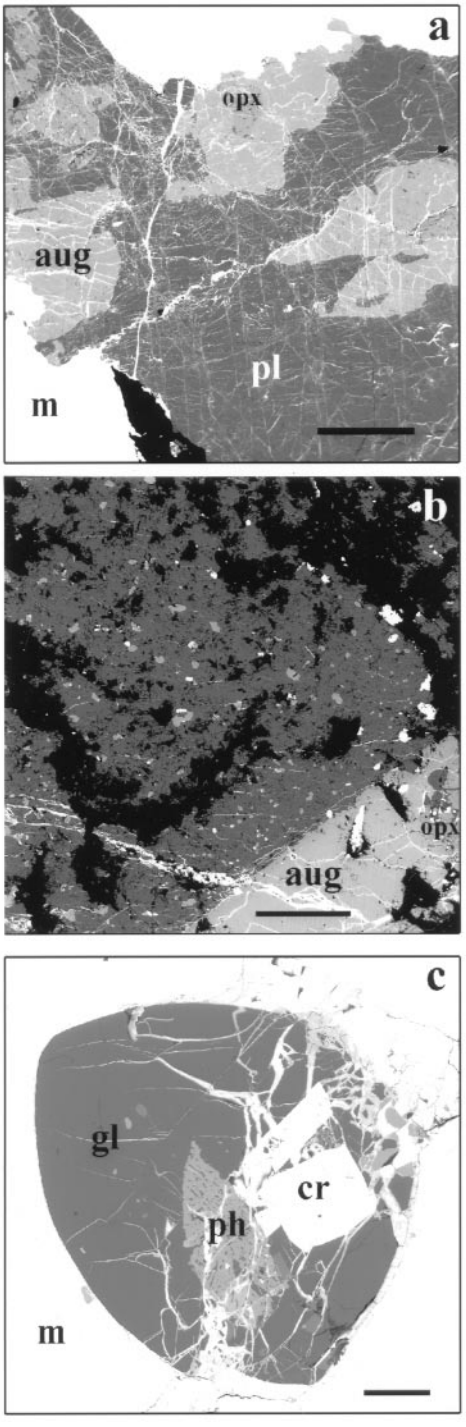

Fig. 2. Backscattered electron images of differentiated silicate inclusions in IIE irons. (a) Gabbroic inclusion in Miles composed of plagioclase (pl), augite (aug), and orthopyroxene (opx) in metal (m). Bright linear features in plagioclase are infilling of planar fractures produced by shock with terrestrial hydrated iron oxides. Scale bar = 500 μm. (b) Partially cryptocrystalline inclusion in Weekeroo Station with a large, euhedral central augite–orthopyroxene grain rimmed by a fine-grained radiating mass of pyroxene, plagioclase, SiO_2, and chromite. Scale bar = 100 μm. (c) Inclusion in Colomera with glassy feldspathic groundmass (gl), skeletal phosphates (ph), and chromite (cr) in metal (m). Scale bar = 100 μm. The meniscus-shaped boundary between the feldspathic glass and phosphates has been suggested as evidence of liquid immiscibility (Buchwald, 1975).

3. RESULTS

3.1. Petrography

In this section, we briefly review the mineralogy, modes, and mineral chemistry of the diverse array of silicate inclusions found in IIE iron meteorites, primarily summarizing the work of others. We report new observations on shock features within the IIE irons.

3.1.1. "Chondritic" inclusions

A number of IIE irons have inclusions that are either chondrule-bearing or roughly chondritic in their mineralogy and mineral abundances. We have studied "chondritic" inclusions in Techado, Netschaevo, and Watson. Chondrule-bearing inclusions also are found in Yamato 791093 (Ikeda et al., 1997a) and Portales Valley (Rubin and Ulff–Moller, 1999), but these meteorites were not included in our study.

Netschaëvo contains angular clasts 1 to 2 cm in length (Fig. 1a), which include recrystallized chondrules typical of those found in type 6 ordinary chondrites (Bunch et al., 1970; Olsen and Jarosewich, 1971; Bild and Wasson, 1977). The silicate mineralogy of these clasts is essentially identical to chondrites (Table 1), containing olivine ($Fa_{14.1}$), orthopyroxene ($Fs_{13.6}$), plagioclase and phosphates, although the clasts are richer in orthopyroxene and phosphates, poorer in olivine, and contain mafic silicates more reduced than found in H chondrites. Olivine in the silicate inclusions exhibits undulatory extinction, healed fractures decorated with opaques or, more commonly, voids, and rare planar fractures. Compound Fe,Ni–FeS–oxide particles exhibit eutectic intergrowths and kamacite has been converted to the α_2 structure (Buchwald, 1975). The features within olivine would suggest classification as shock stage S2-S3 (Stöffler et al., 1991) and postshock temperature increase of 50 to 100°C. However, Netschaëvo was forged shortly after its recovery and locally reheated to temperatures above 1000°C (Buchwald, 1975). The effect reheating to this temperature may have on annealing of shock features is not known.

Casanova et al. (1995) described a single silicate inclusion ~1.5 cm in length from Techado (Fig. 1b). This inclusion is roughly chondritic in bulk mineralogy (Table 1), consisting of olivine ($Fa_{16.4}$), orthopyroxene ($Fs_{15.3}$), plagioclase ($An_{14.9-15.4}$ $Or_{5.6-6.3}$), Fe,Ni metal, and troilite. Although Casanova et al. (1995) suggested that the inclusion was unmelted, it has an unusual elongated shape that suggests that it was heated to temperatures sufficient to cause the inclusion to soften and become stretched. Casanova et al. (1995) suggested that the inclusion was unshocked. Our examination suggests that olivine and orthopyroxene both exhibit planar fractures and undulatory extinction, suggesting classification as S3 (Stöffler et al., 1991) and postshock heating of 100 to 150°C. Neumann bands are also present in the metallic host of Techado.

Olsen et al. (1994) reported a comprehensive study of Watson, including the discovery of a single silicate inclusion of ~30 cm^3 (Fig. 1c). The Watson inclusion is roughly chondritic in bulk composition (Olsen et al., 1994). A calculated modal mineralogy of this inclusion (Olsen et al., 1994; Table 1) contains 57% olivine ($Fa_{20.6}$), 23% orthopyroxene ($Fs_{17.6}Wo_{3.8}$), and 12% feldspar; Fe,Ni metal and troilite are essentially absent. The texture is decidedly non-chondritic and similar to that of a terrestrial

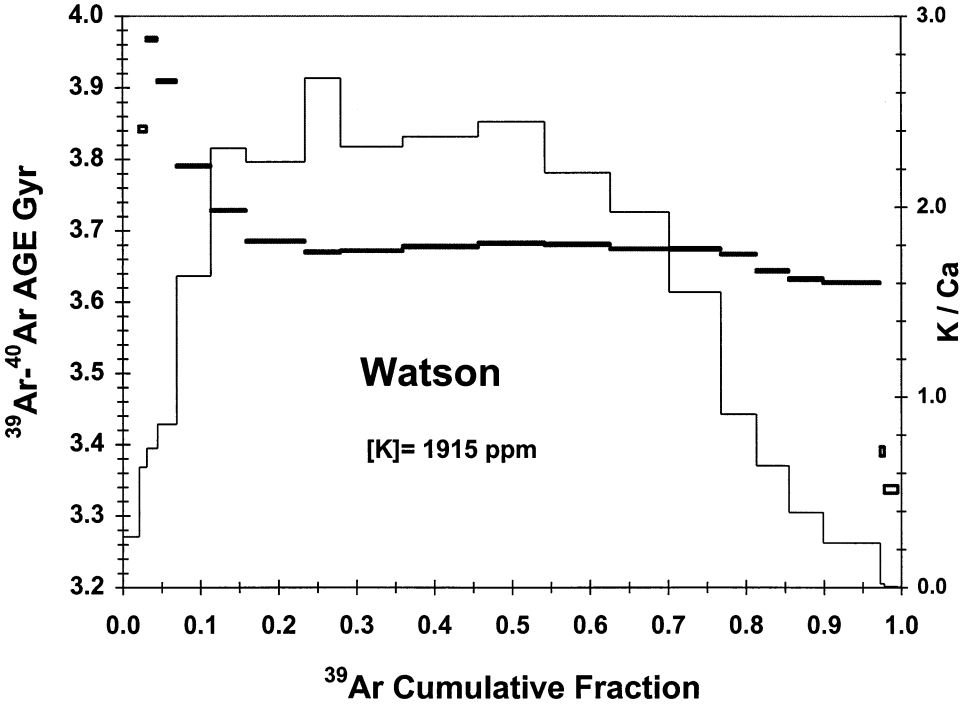

Fig. 3. ^{39}Ar–^{40}Ar ages (rectangles) and K/Ca ratios (stepped line) as a function of cumulative release of ^{39}Ar for stepwise temperature extractions of silicate from the Watson IIE meteorites. Individual age uncertainties are indicated by the widths of the rectangles and include all analytical uncertainties in the $^{40}Ar/^{39}Ar$ ratios (see text for details).

peridotite (Olsen et al., 1994). The silicate inclusion is dominated by orthopyroxene crystals, 0.5 to 2 mm in maximum dimension, which poikilitically enclose olivine crystals. Olsen et al. (1994) noted the presence of dendritic melt pockets, α_2 structure, and Neumann bands within the metallic host. The first two of these suggest brief, local heating to temperatures in excess of 700°C. We have observed a number of other features related to post-formational shock, including shearing of the large inclusion and undulatory extinction and planar fractures in both olivine and pyroxene. These features correspond to shock stage S3 and postshock heating of 100 to 150°C.

3.1.2. Differentiated inclusions

The remaining silicate-bearing IIE irons (Weekeroo Station, Miles, Colomera, Kodaikanal, and Elga) all contain what Prinz et al. (1983) aptly described as globular silicate inclusions. These inclusions are rounded to elongate and typically can reach 1 cm in length and comprise ~10 vol.% of the bulk meteorite (Fig. 1d). Inclusions in Weekeroo Station and Miles are dominantly orthopyroxene, clinopyroxene and plagioclase in a ratio of 1:1:2, whereas Colomera, Kodaikanal, and Elga inclusions contain major clinopyroxene and plagioclase (~1:2 or 1:3) with only minor orthopyroxene (Table 1). These inclusions have been studied by Bunch and Olsen (1968), Wasserburg et al. (1968), Bence and Burnett (1969), Bunch et al. (1970), Olsen and Jarosewich (1970), Osadchii et al. (1981), Prinz et al. (1983), and Ikeda and Prinz (1996). Silicate inclusions in the ungrouped irons Guin (Rubin et al., 1985) and Sombrerete (Prinz et al., 1982) are similar to the differentiated inclusions in group IIE irons.

Weekeroo Station, Miles, Colomera, Kodaikanal, and Elga contain: 1) coarse-grained (up to 5 mm grain size) gabbroic inclusions (Fig. 2a); 2) partially to wholly cryptocrystalline inclusions (Fig. 2b); and 3) glassy inclusions (Fig. 2c). The ratio of these types can differ significantly. In Miles, most inclusions are gabbroic (Ikeda and Prinz, 1996; Ikeda et al., 1997b), whereas most inclusions in Weekeroo Station and Elga are at least partially cryptocrystalline. Glassy inclusions are found in Colomera and Kodaikanal. Gabbroic inclusions in Miles consist of 1 to 5 mm grains of feldspar (both plagioclase and potassium feldspar), augite ($Fs_{8-12}Wo_{40-45}$), and orthopyroxene (Fs_{19-23}; Ikeda and Prinz, 1996; this work). Millimeter-sized chromite grains are also found in the gabbroic inclusions. Grain boundaries are irregular and often interfinger. Cryptocrystalline inclusions are typified by the corona structure found in Weekeroo Station (Bunch et al., 1970) with a large (up to several mm) corroded augite ($Fs_{17.6}$) rimmed by orthopyroxene ($Fs_{22.2}$; Bunch et al., 1970) and surrounded by a fine-grained radiating structure of acicular feldspar, tridymite, and glass. Ikeda et al. (1997b) illustrated an almost identical structure in Miles. Colomera contains these two types of inclusions, as well as glassy inclusions (Buchwald, 1975). In some areas, we have observed that all three types of inclusions can be found co-existing in an area of ~1 cm^2, well below the heat-altered zone of the meteorite. The glasses tend to be feldspathic in nature (this work) and often contain immiscible phosphate-rich melts (Buchwald, 1975).

Shock features are abundant within IIE irons with differentiated silicate inclusions. Buchwald (1975) reported violently deformed Neumann bands, fractured schreibersite and shock-

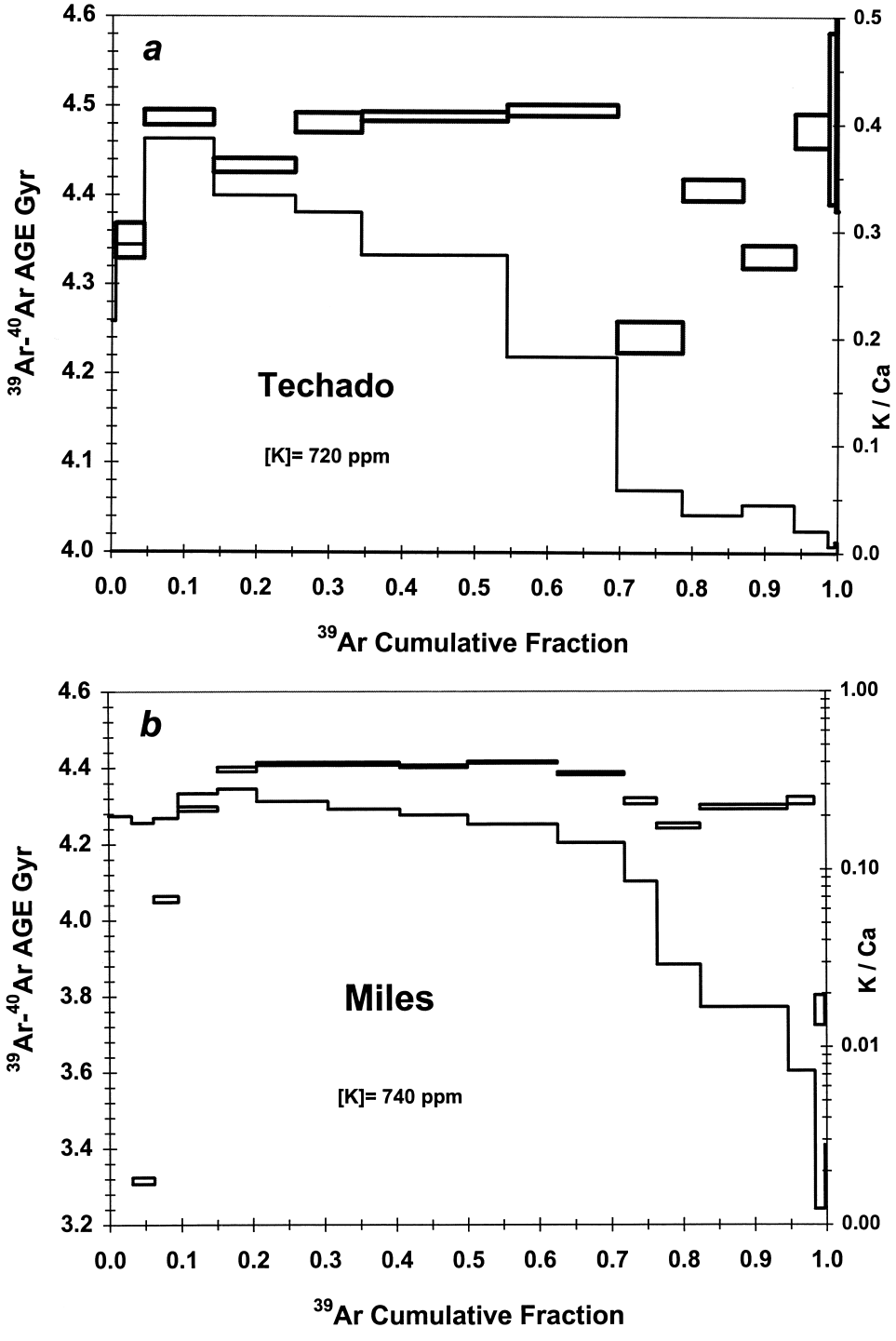

Fig. 4. ^{39}Ar–^{40}Ar ages (rectangles) and K/Ca ratios (stepped line) as a function of cumulative release of ^{39}Ar for stepwise temperature extractions of: (a) Techado, (b) Miles, (c) Colomera feldspar, and (d) Sombrerete.

melted troilite in the vicinity of silicate inclusions in Colomera and fracturing of schreibersite and dispersion of troilite in Weekeroo Station. Kodaikanal has experienced even more substantial deformation, including shearing and micromelting (Buchwald, 1975). We have observed a variety of shock features in the silicates of Miles, Colomera, Kodaikanal, and Weekeroo Station. These include deformation twins, planar fractures, and undulatory extinction in pyroxene, and planar fractures and undulatory extinction in large plagioclase grains. These features correspond to shock stage S4 and postshock heating of ~300°C. As we discuss later, it is possible that the fine-grained radiating structures and glassy structures with multiple, immiscible liquids also formed as a result of shock, as argued by Osadchii et al. (1981).

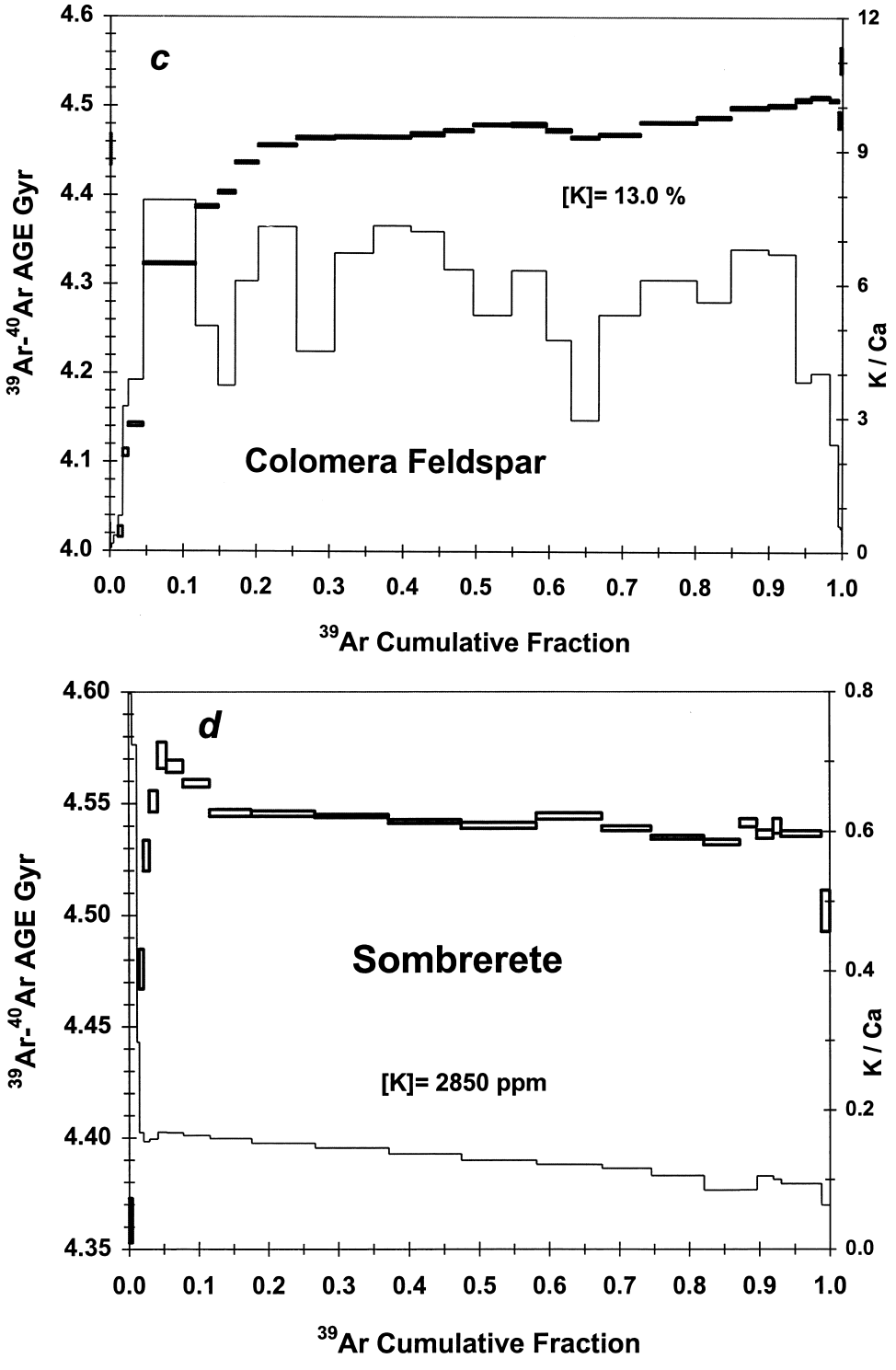

Fig. 4. (Continued)

3.2. ^{39}Ar–^{40}Ar Chronologies

The ^{39}Ar–^{40}Ar ages and K/Ca ratios as a function of cumulative release of ^{39}Ar for the five irradiated meteorite samples are shown in Figures 3 and 4a–d. Age uncertainties for individual extractions shown in the figures represent only analytical uncertainties in determining the ^{40}Ar/^{39}Ar ratio. However, uncertainties reported for Ar–Ar "plateau" ages are determined from variations among individual extraction ages and the uncertainty in J (see Section 2). Here we discuss some of the characteristics of these age spectra and present our preferred Ar–Ar age for each meteorite. In Section 4, we compare these

Table 2. Radiometric ages of IIE meterorites.

Meteorite	Radiometric Age, Gyr	Method	Ref.[c]
Watson	3.676 ± 0.007	Ar–Ar	(a)
	3.5 ± 0.2	K–Ar	(b)
	3.0	Sm–Nd[a]	(c)
Kodaikanal	3.676 ± 0.003	Pb–Pb	(d)
	3.7 ± 0.1	Rb–Sr[b]	(e)
	~3.4	K–Ar	(f)
	~4.62	Re–Os	(g)
Netschaëvo	3.74_5 ± 0.03	Ar–Ar	(h)
Colomera	4.470 ± 0.010	Ar–Ar	(a)
	4.51 ± 0.04	Rb–Sr[b]	(i)
Sombrerete	4.541 ± 0.012	Ar–Ar	(a)
Weekeroo Station	4.49 ± 0.03	Ar–Ar	(h)
	4.3 ± 0.1	K–Ar	(j)
	4.555	I–Xe	(k)
	4.28 ± .23–.12	Rb–Sr[b]	(l)
	4.39 ± 0.07	Rb–Sr	(m)
	0.7	Sm–Nd[a]	(c)
Miles	4.408 ± 0.009	Ar–Ar	(a)
	4.27	Sm–Nd[a]	(c)
Techado	4.489 ± 0.013	Ar–Ar	(a)
	~4.6	K–Ar	(n)

K–Ar and Rb–Sr ages are calculated using the decay parameters recommended by Steiger and Jäger (1978). See text for explanation of uncertainties for new Ar–Ar ages reported here.

[a] Sm–Nd model ages, not isochron ages.

[b] Rb–Sr ages recalculated using $\lambda = 1.42 \times 10^{-11}$. All Rb–Sr ages would be older by 1.3% using $\lambda = 1.402 \times 10^{-11}$.

[c] (a) This work; (b) Olsen et al., 1994l (c) Synder et al., 1998; (d) Göpel et al., 1985; (e) Burnett and Wasserburg, 1967a; (f) Bogard et al., 1969; (g) Birck and Allègre, 1998; (h) Neimeyer, 1980; (i0 Sanz et al., 1970; (j) Bogard et al., 1968; (k) Brazzle et al., 1999; (l) Burnett and Wasserburg, 1967b; (m) Evensen et al., 1979; (n) Casanova et al., 1995.

new Ar–Ar ages with previous radiometric ages of these meteorites, where such data exists. Table 2 summarizes our preferred Ar–Ar age for each meteorite analyzed along with literature data on IIEs.

3.2.1. Watson

The release profiles of ^{39}Ar–^{40}Ar ages and K/Ca ratios for the whole rock sample of Watson (Fig. 3) suggest significant amounts of recoil redistribution of ^{39}Ar among phases. When ^{39}Ar is produced in the reactor by the n,p reaction on ^{39}K it undergoes a recoil of ~0.16 μm (Onstott et al., 1995), which can produce a net transfer of ^{39}Ar from grain surfaces with higher K to those with lower K. In Watson, changes in the K/Ca ratio and Ar–Ar ages with temperature show three "regimes" at ~0 to 17%, ~17 to 82%, and >82% of the total ^{39}Ar release, indicating that three different structural or mineral "phases" control the release of ^{39}Ar, ^{40}Ar, and ^{37}Ar. We attribute the peak in Ar–Ar ages at ~2 to 17% of the ^{39}Ar release to recoil loss of ^{39}Ar from surfaces of K-rich grains, and the lower Ar–Ar ages at >82% ^{39}Ar release to gain of this recoiled ^{39}Ar by phases with lower K/Ca ratios. This redistribution of recoiled ^{39}Ar between phases causes the apparent Ar–Ar ages to increase and decrease for lower and higher temperature extractions, respectively. (The lower age for the first extraction [0 to 2% ^{39}Ar release] we attribute to diffusive loss of ^{40}Ar). Olsen et al. (1994) describe the clear feldspar in Watson as an antiperthite consisting of fine exsolution lamellae of orthoclase-rich feldspar (with [K] = 5.7% and a K/Ca ratio of ~28) that have exsolved from albitic feldspar. The K/Ca of the albite is ~2.3. The average K/Ca of extractions with ^{39}Ar releases of ~11 to 70% is also 2.3. The bulk K/Ca ratio of 0.14 reported for Watson by Olsen et al. (1994) is nearly identical to our overall ratio of 0.16. Pyroxenes in Watson are variable in composition, but some have Ca concentrations as large as ~13.5% and vanishingly small K/Ca ratios (Olsen et al., 1994). It is the juxtaposition of phases with such extreme K/Ca ratios that produces the relatively large Ar recoil effects in Watson.

That Ar which degassed over nine extractions between ~15 to 81% of the total ^{39}Ar release, gives a constant Ar–Ar "plateau" age of 3.676 ± 0.007 Gyr. The deficiency of ^{39}Ar in the 2 to 15% release (relative to the plateau age) is equal to the excess of ^{39}Ar in the 81 to 100% release (within a few percent), and indicates that ^{39}Ar was not lost from the bulk sample during recoil. This agreement implies that the "plateau" age in the middle portion of the ^{39}Ar release, which derives from the interiors of feldspar grains, was not affected by ^{39}Ar recoil redistribution. Thus, we interpret the 3.676 Gyr age to be the time of last major Ar degassing of Watson silicate. The total ^{39}Ar–^{40}Ar age for this Watson sample (summed over all extractions except the first) has an identical value of 3.677 Gyr. This agreement of total and plateau ages suggests that little radiogenic ^{40}Ar has been lost since the ~3.68 Gyr resetting event.

3.2.2. Techado

Silicate from Techado whole rock contains K at chondritic levels. The K/Ca ratio decreases throughout the extraction and suggests overlap in Ar degassing from at least two different lattice sites (Fig. 4a). The first two extractions and some extractions above ~70% of the total ^{39}Ar release show slightly lower Ar–Ar ages and suggest diffusive loss of radiogenic ^{40}Ar, possibly from weathered grain surfaces. Alternatively, these Ar releases may show gain of recoil ^{39}Ar, but the source of such recoil ^{39}Ar is not apparent in the low-temperature releases (e.g., compare with Watson). The total Ar–Ar age is 4.43 Gyr. The age obtained by omitting the first two extractions and the one extraction at ~70 to 78% ^{39}Ar release (the lower age of which has no obvious explanation) is 4.46 Gyr. We consider 4.46 Gyr to be a lower limit to the K–Ar age. Four of five extractions releasing ~5 to 70% of the ^{39}Ar from Techado suggest an ^{39}Ar–^{40}Ar plateau age of 4.489 ± 0.013 Gyr. This value is probably closer to the actual K–Ar age.

3.2.3. Miles

Both changes in the K/Ca ratio (Fig. 4b) and the rate of ^{39}Ar release from Miles suggest that a phase with constant K/Ca releases Ar up to ~75% of the total ^{39}Ar, followed by Ar release from phases with much lower net K/Ca. Grain sites releasing between ~0 to 15% of the total ^{39}Ar indicate some prior diffusive loss of radiogenic ^{40}Ar. Six extractions releasing over ~15 to 72% of the total ^{39}Ar give a plateau age of 4.405 ± 0.012 Gyr, and four extractions releasing over ~20 to 62% of the total ^{39}Ar give an age of 4.408 ± 0.009 Gyr. The phases

Table 3. Isotopic abundances (in units indicated of cm^3STP/g) of He, Ne, and Ar.

Sample °C	^{3}He 10^{-8}	^{4}He 10^{-6}	^{22}Ne 10^{-8}	$^{21}Ne_{cos}$ 10^{-8}	$^{20}Ne/^{22}Ne$	$^{21}Ne/^{22}Ne$	^{36}Ar 10^{-8}	^{40}Ar 10^{-5}	$^{38}Ar_{cos}$ 10^{-8}	$^{38}Ar/^{36}Ar$
Miles										
400	0.32	5.4	2.1	1.28	0.587 + .025	0.629 + .002	0.07	0.13	0.02	2.43 + .21
1550	1.93	23.8	56.9	56.7	0.881 + .001	1.026 + .001	7.31	3.85	10.78	0.677 + .001
Total	2.247	29.1	59.0	58.0		1.012	7.38	3.98	10.8	
Netschaevo										
400	0.02	0.29	0.02	0.02	2.029 + 0.60	0.880 + .015	0.05	0.03	0.06	0.876 + .120
1550	0.94	0.79	0.98	0.96	0.866 + .015	1.011 + .004	0.41	1.13	0.10	2.445 + .022
Total	0.96	1.08	1.00	0.98		1.008	0.46	1.16	0.16	
Sombrerete										
400	9.1	1.9	0.1	0.1	0.836 + .185	0.735 + .023	0.34	0.1	0.31	1.013 + .009
1550	276.1	39.8	59.2	57.4	0.866 + .001	1.000 + .001	54.3	16.5	61.0	0.855 + .001
Total	285.2	41.7	59.3	57.5		0.999	54.7	16.6	61.3	
Colomera feldspar										
400	0.75	0.69	0.02	0.01	4.19 + 1.75	0.425 + .131	0.3	2.26	0.18	1.405 + .031
1550	12.23	7.82	7.93	7.54	0.886 + .017	0.980 + .002	25.85	n.m.	45.14	0.583 + .001
Total	12.98	8.51	7.95	7.55		0.979	26.15		45.32	

Calculated concentrations of cosmogenic ^{21}Ne and ^{38}Ar are also given. Uncertainties are indicated below each isotopic ratio. Absolute abundances are estimated at ±5–10%.

*Given are 400°C and 1550°C extractions of unirradiated samples of IIE silicate.

with lower K/Ca degassing Ar at higher temperatures show slightly lower Ar–Ar ages. We interpret this decrease in age to be caused by gain of recoiled ^{39}Ar, the source of which was in the low-temperature phase that has lost ^{40}Ar. The total age above 15% ^{39}Ar release is 4.38 Gyr and is probably a firm lower limit to the time of last resetting of the K–Ar age.

3.2.4. Colomera

For the sample of Colomera feldspar, the K/Ca ratio is relatively constant across most of the Ar release but shows an unusual amount of fine-scale variation (Fig. 4c). No obvious features of ^{39}Ar recoil redistribution exist in the age spectrum. Modest diffusive loss of radiogenic ^{40}Ar is indicated over 0 to 25% of the total ^{39}Ar release. The average ^{39}Ar–^{40}Ar age for all extractions above 25% ^{39}Ar release is 4.48 Gyr. However, the Ar–Ar ages tend to increase with increasing ^{39}Ar release. This increase in age is much larger than the typical uncertainty in individual ages of ~1 Myr, as calculated from the uncertainty in ^{40}Ar/^{39}Ar alone (Appendix 1). Ten extractions releasing over ~25 to 72% of the total ^{39}Ar release give an age of 4.470 Gyr, with an uncertainty of 4.5 Myr considering only variations among individual ages, and an uncertainty of 10 Myr considering the additional uncertainty in *J*. On the other hand, the last several extractions show ages up to ≥4.50 Gyr, and the average age for seven extractions comprising the last 15% of the ^{39}Ar release is 4.50 ± 0.02 Gy. (The 1550°C extraction, not included in the above average, released only 0.05% of the ^{39}Ar and had significant blank corrections.) We have observed similar sloped Ar–Ar age spectra in mesosiderites (Bogard and Garrison, 1998) and in silicate from the Caddo County IAB iron (Takeda et al., 2000), and we interpret these as arising from the K–Ar chronometer being partially open during relatively slow cooling within the parent body. Alternatively, the original K–Ar age of Colomera feldspar may have been >4.5 Gyr, and was partially reset during impact heating ~4.47 Gyr ago.

3.2.5. Sombrerete

Both the K/Ca ratio and Ar–Ar age spectra for Sombrerete silicate are relatively constant with extraction temperature (Fig. 4d). A small amount of diffusive loss of radiogenic ^{40}Ar is indicated for the first few extractions, which have higher K/Ca ratios. Three extractions at ~3 to 11% ^{39}Ar release show a small peak in age and indicate that ~0.1% of the total ^{39}Ar has experienced recoil loss. The lower age of the 1550°C extraction suggests that it gained recoiled ^{39}Ar, but this extraction does not contain all of the ^{39}Ar that apparently recoiled. The total ^{39}Ar–^{40}Ar age considering all extractions is 4.536 Gyr. The summed Ar–Ar age over those 13 extractions (775–1350°C) suggesting an age plateau, and releasing 87% of the total ^{39}Ar, is 4.541 ± 0.012 Gyr. The uncertainty in irradiation constant *J* contributes much more to this age uncertainty than does variation in individual Ar–Ar ages. We conclude that no significant ^{40}Ar loss occurred from Sombrerete during the last 4.54 Gyr.

3.3. Space Exposure Ages

Literature data on cosmogenic noble gases in IIE meteorites are sparse. Table 3 presents our results on He, Ne, and Ar released in 400°C and melt (1550°C) extractions of unirradiated silicate samples from Netschaëvo, Sombrerete, Miles, and Colomera feldspar. We examined the cosmic-ray (space) exposure ages of IIE meteorites to determine if the three meteorites with the youngest radiometric ages of ~3.67 Gyr had different exposure ages compared to the other IIEs, as previously suggested by Casanova et al. (1995). If that were the case, it might be suggestive of derivation of the three young IIEs from a different part of the parent body via a different impact event. General experimental techniques are described in Garrison and Bogard (1998). Space exposure ages for these four meteorites, along with literature data for additional IIE meteorites, are estimated in Table 4.

Table 4. Approximate space exposure ages (Ma) of IIE meteorites.

Meteorite	^{3}He	^{21}Ne	^{38}Ar	Reference
Watson (s)	8.2	8.5	7.9	Olsen et al., 94
Kodaikanal (m)	12	15	15	Bogard et al., 69
Netschaëvo (s)	(0.6)	3.0	3.6	This study
	—	—	18	Niemeyer, 80
Colomera (s)	(7)	35	103/27	This study
Sombrerete (s)	165	278	553/819	This study
Weekeroo Sta. (m)	565	530	665	Bogard et al., 69
Weekeroo Sta. (s)			350–410	Niemeyer, 80
Miles(s)	130	215	85/218	This study
Techado (s)	64	56	27	Casanova et al., 95
Techado (m)			60–80	Casanova et al., 95

(s) silicate phase; (m) metal phase. New ages for Netschaëvo were calculated using H-chondrite production rates. HE-3 ages in parenthesis reflect diffusion loss. The two ^{38}Ar ages listed for Sombrerete and Miles were calculated using different values for the Ca concentration. The second values using Ca determined on irradiated samples is preferred. The two ^{38}Ar ages listed for Colomera feldspar assume different production ratios from K and Ca target elements, and the lower age calcualted from p(K)/P(Ca) = 7 is preferred. See Appendix 2 for details.

3.3.1. *Cosmogenic production rates*

Calculation of space exposure ages for most of these IIE meteorites is not straightforward because of uncertainties in the production rates of the cosmogenic noble gases. The ^{21}Ne and ^{38}Ar production rates depend on three major factors: the effects of sample shielding; the chemical composition of the meteorite; and assumptions made about the relative importance of various elements in producing cosmogenic gases. Cosmogenic ^{3}He is much less sensitive to variations in chemistry and shielding, but sometimes it is lost from the meteorite by diffusion.

Shielding differences among samples are often normalized by using the cosmogenic ^{21}Ne/^{22}Ne ratio. Values of this ratio for the four silicate analyses reported here were 0.98 to 1.01. The 400°C extractions give substantially lower ^{21}Ne/^{22}Ne than the melt extractions, probably due to preferential release of Ne produced from low-energy reactions on Na. However, the 400°C concentrations are small compared to the total Ne amounts. The total ^{21}Ne/^{22}Ne ratios measured for all four meteorites are significantly larger than those expected or observed in even the largest ordinary chondrites (Graf et al., 1990; Garrison et al., 1992). Similar ^{21}Ne/^{22}Ne ratios of ~1 are observed in silicates from mesosiderites and some other iron meteorites and have been attributed to an enhanced production of secondary neutrons over secondary protons in the metal matrix (Jentsch and Schultz, 1996). Such an effect makes it difficult to use ^{22}Ne/^{21}Ne as a shielding indicator. Consequently, we made no shielding corrections to the IIE silicate data.

Another possible source of error in deriving cosmogenic production rates for IIE silicates derives from uncertainties in the chemical composition of the samples and from the elemental production rates assumed. Largely because of the different degrees of differentiation in IIE silicates, especially regarding metal, their chemical compositions and thus the cosmogenic production rates are variable. On the other hand, the high K/Ca ratio in Colomera feldspar presents an opportunity to further define the relative importance of K and Ca to production of cosmogenic ^{38}Ar. For a detailed discussion of how we derived the cosmogenic production rates used to calculate IIE exposure ages, the reader is referred to Appendix 2. We also discuss in Appendix 2 possible reasons for some of the apparent differences in various exposure ages calculated for the same meteorite.

3.3.2. *Comparison of IIE exposure ages*

Watson, Kodaikanal, and Netschaëvo all have relatively short space exposure ages (Table 4). These ages are similar to those for many H-chondrites, which show a strong exposure age peak at 5 to 10 Myr (Graf and Marti, 1995), as pointed out by Olsen et al. (1994) for Watson. Given the uncertainties in sample composition and shielding, the exposure ages of Watson and Kodaikanal could be the same. The exposure age for Netschaëvo, ~3 Myr, seems distinctly younger, but we cannot rule out the possibility of extreme shielding, a secondary breakup in space, or diffusive loss of gases during forging. These three IIE meteorites also all have young radiometric ages (Table 2), and it is likely (but not required) that they were ejected from a single locale on their parent body by a single cratering event. The other five IIE meteorites indicate a spread of space exposure ages that are all considerably older. Exposure ages for Colomera and Techado are probably at least ~35 Myr, and the Weekeroo Station age is probably several hundred Myr. Thus, we suggest that in addition to their young radiometric ages, Watson, Kodaikanal, and Netschaëvo also may possess the common characteristic of having been derived from a different portion of the IIE parent body compared to other IIE meteorites. Niemeyer (1980) suggested a different parent body altogether. This may be a factor in why these three meteorites alone among the IIEs show reset isotopic ages. These young IIE exposure ages also are lower than ages for other silicate-bearing iron meteorites. For example, Niemeyer (1979) calculated ^{38}Ar exposure ages of ~130 to 480 Ma for silicate from several IAB meteorites by using Ar measured in irradiated samples and an assumed production rate of 2.4×10^{-8} cm^3/g Ca/Myr.

3.4. Cosmogenic Xenon

Xenon in the melt extractions of four IIE silicate samples (Table 5) contains a cosmogenic component. (Smaller Xe amounts released in the 400°C extractions were apparently dominated by terrestrial Xe and were not measured in detail.) We assume that the dominant trapped Xe component in these meteorites has the composition of CI chondrites (Pepin, 1991). To derive the cosmogenic Xe spectrum, we normalize the measured Xe isotopic composition to ^{136}Xe and subtract out this trapped component, assuming all ^{136}Xe is trapped. The isotopic composition of this cosmogenic Xe, normalized to ^{126}Xe = 1, is plotted in Figure 5 for the three IIE samples that showed the largest cosmogenic excesses. ^{129}Xe is not plotted because of the obvious presence in Sombrerete and Colomera of ^{129}Xe from the decay of extinct ^{129}I. Uncertainties indicated in Xe data for Sombrerete and Colomera are derived from uncertainties in blank corrections and ratio measurements, propagated through ratio normalization. The uncertainties in Figure 5 appear relative large for larger Xe masses because the

Table 5. Abundances of ^{132}Xe (10^{-12} cm^{3}STP/g) and relative Xe isotopic composition (^{132}Xe = 1.00) of IIE silicate.

	^{132}Xe 10^{-12} cc/g	136 ±	134 ±	132	131 ±	130 ±	129 ±	128 ±	126 ±	124 ±
Sombrerete	3.85	0.267	0.314	≡1.0	1.434	0.395	4.423	0.481	0.232	0.122
	1.64	0.013	0.005		0.032	0.007	0.106	0.011	0.006	0.007
Colomera feldspar	28.4	0.273	0.392	≡1.0	1.238	0.295	2.011	0.357	0.179	0.086
	22.9	0.030	0.030		0.093	0.023	0.122	0.027	0.012	0.018
Miles	4.12	0.323	0.387	≡1.0	1.203	0.207	1.092	0.241	0.107	n..m.
	76.7	0.035	0.054		0.164	0.064	0.120	0.051	0.028	
Netschaevo	17.3	0.319	0.376	≡1.0	0.843	0.171	1.123	0.083	n.m.	n.m.
	30.1	0.012	0.009		0.021	0.010	0.033	0.005		
AVCC (Pepin, 1991)		0.275	0.352	≡1.0	0.826	0.165	1.040	0.084	0.0042	0.0049

Two ^{132}Xe abundances are given for each sample. The first is the 400°C extraction, and the second is the melt extraction. Isotopic abundances are from the melt extraction, and the uncertainties for these are given below each isotope.

spallation spectrum is derived by taking a relatively small difference between measured and AVCC compositions. Xe data for Miles has even larger uncertainties, which are not plotted. Residual excesses in ^{134}Xe are small and could represent uncertainties in the composition of the assumed trapped component. Also plotted in Figure 5 are the cosmogenic Xe spectra reported for the Weekeroo Station IIE (Bogard et al., 1971a) and the Stannern eucrite (Marti et al., 1966).

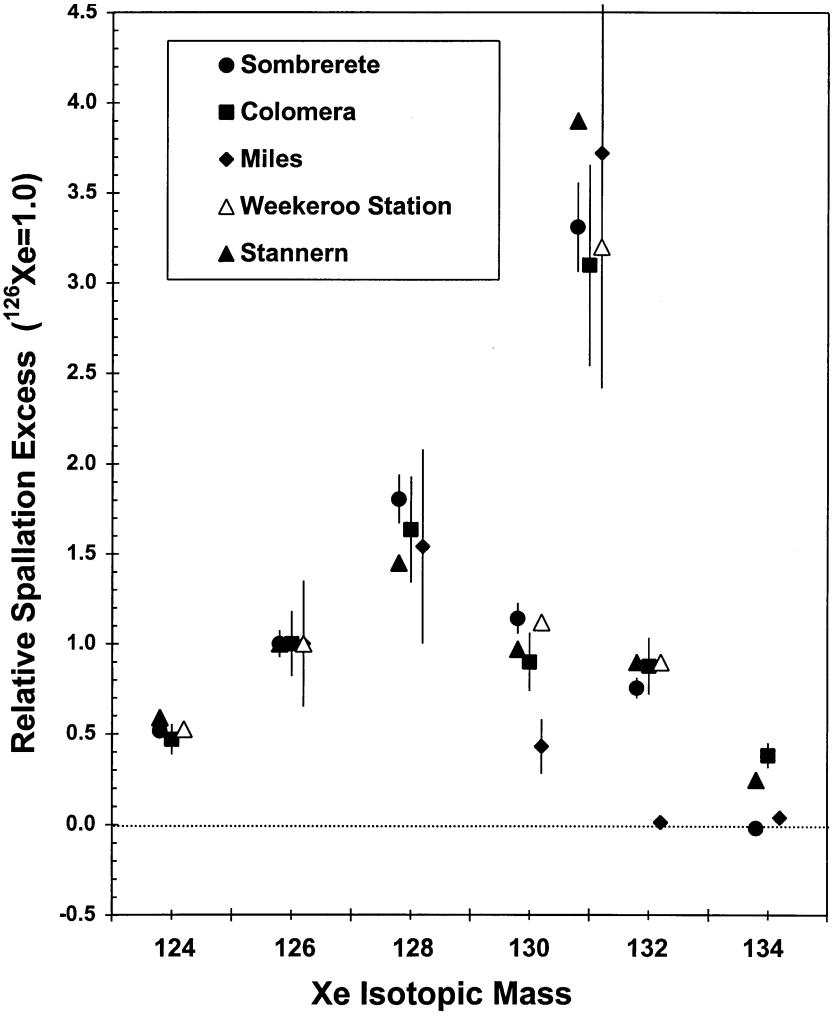

Fig. 5. Comparison of relative isotopic concentrations of cosmogenic Xe in Sombrerete, Colomera feldspar, and Miles (this study); in Weekeroo Station (Bogard et al., 1968); and in the Stannern eucrite (Marti et al., 1966). A trapped Xe component with the composition of AVCC Xe has been subtracted, and the cosmogenic spectrum is normalized to ^{126}Xe = 1. Uncertainties are indicated for Sombrerete and Colomera, and are even larger for Miles.

The plotted cosmogenic Xe spectra for the IIEs are generally similar, especially at masses 124 to 130, where uncertainties are relatively small. Differences in spallation Xe shown by Miles at masses 130 and 132 are not significant given the relative large uncertainties on these data. The relative production of cosmogenic ^{131}Xe can be enhanced under large shielding conditions due to thermal neutron capture by ^{130}Ba. Because IIE silicates were irradiated in an extensive matrix of metal, and because Fe is a strong absorber of epithermal neutrons, we might expect that the relative yield of cosmogenic ^{131}Xe would be lower in IIE silicate than in other silicate samples irradiated under moderate shielding. The relative yield of ^{131}Xe is slightly larger in the Stannern eucrite compared to the IIE meteorites, although the differences generally lie within uncertainties. However, lunar regolith samples, which were irradiated under a wide range of shielding conditions, give considerably larger cosmogenic ^{131}Xe/^{126}Xe of ~4 to 8 (Bogard et al., 1971b). We suggest that the value of cosmogenic ^{131}Xe/^{126}Xe of ~3.3 observed in three IIE samples characterizes irradiation under relatively large shielding and is an approximate lower limit to cosmogenic Xe produced in the absence of a significant thermal neutron capture component.

4. COMPARISON OF IIE RADIOMETRIC AGES

Little precise age data existed for the meteorites analyzed here when we began our study. Among reported data are classical K–Ar ages for Watson and Techado, an older Rb–Sr isochron age for Colomera, and model-dependent, whole-rock Sm–Nd ages for single inclusions from Watson and Miles (Table 2). To our knowledge, no isotopic ages have been reported for Sombrerete. Isotopic ages have been reported for silicate from some other IIE iron meteorites. These include ^{39}Ar–^{40}Ar ages for Weekeroo Station and Netschaëvo, classical K–Ar ages for Weekeroo Station, and two determinations of the Rb–Sr isochron age of Weekeroo Station (Table 2). In addition, Niemeyer (1980) reported a I–Xe age for Weekeroo Station that is 11 Myr younger than Bjurböle and several Myr younger than I–Xe ages on silicate from some IAB iron meteorites. Several age determinations on Kodaikanal (Table 2) include a classical K–Ar age, two determinations of the Rb–Sr isochron age, and a Pb–Pb age (^{238}U–Pb, and ^{235}U–Pb ages are similar). The Rb–Sr data for Kodaikanal indicate that chemical fractionation occurred at this time. On the other hand, ^{187}Re–^{187}Os data for Kodaikanal metal lie on the same 4.6 Gyr isochron as several other iron meteorites (Birck and Allègre, 1998) and suggest that the Re-Os chronometer was not reset. Analysis of tungsten isotopes in Watson metal also indicates that the short-lived ^{182}Hf–^{182}W chronometer was not reset by the ~3.7 Gyr event (Snyder et al., 1998). In addition to these IIE ages, silicates from five IAB iron meteorites gave ^{39}Ar–^{40}Ar ages of 4.45 to 4.53 Gyr (Niemeyer, 1979; Takeda et al., 1999).

4.1. Young Age Group

Radiometric ages of silicate from three IIE meteorites, Watson, Kodaikanal, and Netschaëvo (determined by three techniques in the case of Kodaikanal), are ~3.67 to 3.75 Gyr (Table 2). In addition, Niemeyer (1980) found a lack of I–Xe correlation for Netschaëvo, consistent with an age younger than ~4.45 Gyr. Among the three most precise ages (the Ar–Ar ages for Watson and Netschaëvo and the Pb–Pb age for Kodaikanal), the ages for Watson and Kodaikanal are identical, but the Netschaëvo age is slightly higher. An important question is whether these younger ages are the same, indicating resetting of all three meteorites in a common event, or require separate events. The two Ar–Ar ages depend on the accuracy of the age of a standard sample irradiated with the IIE samples, and these standard samples were different for Watson and Netschaëvo. We compare the likely accuracy of these two standards in Appendix 3. We conclude that the uncertainty in the Ar–Ar age of the St. Severin irradiation monitor is sufficiently great such that the uncertainty in the Ar–Ar age of Netschaëvo likely overlaps the 3.676 Gyr Ar–Ar age for Watson.

Thus, we conclude that it is likely (but not required) that the Watson, Kodaikanal, and Netschaëvo IIE silicates have exactly the same radiometric age of ~3.676 Gyr and were reset by a common event. The older Re–Os age for Kodaikanal metal and the W isotopic data for Watson metal demonstrate that the metal in IIEs formed early and did not equilibrate with silicate during the process that produced the younger ages of three of the IIEs. However, because Re and Os essentially are taken up only by metal, even during significant secondary heating, the Re–Os age of Kodaikanal is not sensitive to silicate resetting (Birck and Allègre, 1998).

4.2. Old Age Group

Silicate from the other five IIE meteorites all show much older radiometric ages of ≥4.27 Gyr (Table 2). The reported Ar–Ar ages for Colomera, Techado, and Weekeroo Station and the Rb–Sr age for Colomera overlap within their respective uncertainties. The Ar–Ar "plateau" age for Colomera appears slightly younger than its Rb–Sr age, but the Ar–Ar age observed in high temperature extractions is nearly the same as the Rb–Sr age. However, it seems doubtful that the K–Ar age of all five meteorites with old ages (Colomera, Techado, Weekeroo Station, Sombrerete, and Miles) all closed at the same time. The Ar–Ar ages reported here for these five meteorites suggest an age spread of ~0.13 Gyr, with Sombrerete being the oldest and Miles the youngest. Further, from Sr isotopic data Sanz et al. (1970) suggested possible evolutionary histories of Colomera and Weekeroo Station. Assuming evolution in a simple system with chondritic Rb/Sr ≅ 0.26, they concluded that Colomera probably isotopically equilibrated ~40 Myr after the time such a system would have a ^{87}Sr/^{86}Sr intercept equal to BABI; which is an average value for eucrites. The time when ^{87}Sr/^{86}Sr = BABI may be given by precise Pb–Pb ages of 4.556 to 4.560 determined for the Ibitira eucrite (Chen and Wasserburg, 1985; Manhes et al., 1987). Thus, the time when ^{87}Sr/^{86}Sr evolution in a chondritic system would equal that measured in Colomera would be ~4.52 Gyr (assuming $\lambda^{87}\text{Rb} = 1.42 \times 10^{-11}$). Similarly, Evensen et al. (1979) noted that the Rb–Sr age and initial ^{87}Sr/^{86}Sr intercept of Weekeroo Station also would be consistent with simple evolution in a system with chondritic Rb/Sr. In comparing ^{87}Sr/^{86}Sr among several different Colomera inclusions, Sanz et al. (1970) found no direct evidence for later Sr equilibration. However, they stated that Sr equilibration could have occurred up to ~0.03 Gyr after silicate formation. The slightly younger Ar–Ar age could indicate that

Colomera cooled sufficiently slowly that the Ar–Ar system remained partially open to diffusion for a period of ~0.04 Gyr after the Rb–Sr system closed. These considerations suggest that temperatures sufficient to prevent closure of isotopic chronometers existed in parts of the IIE parent body for significant periods of time, which is consistent with petrologic data suggesting relatively slow cooling for differentiated silicates.

The various radiometric ages for Weekeroo Station present something of an enigma. The Weekeroo Station Ar–Ar age, which should be more easily reset, is slightly older than the two Rb–Sr ages. However, the combined uncertainties on these three ages are sufficiently large to be consistent with a single age. If we assume $\lambda^{87}Rb = 1.402 \times 10^{-11}$, as suggested by Birck and Allègre (1978) and Minster et al. (1982), the two determined Rb–Sr ages for Weekeroo Station become 4.34 Gyr and 4.45 ± 0.03Gyr, in better agreement with the Ar–Ar age. However, the Rb–Sr age for Colomera would then rise to 4.57 ± 0.04 Gyr, and the age uncertainty does not quite permit Colomera to be ~40 Myr younger than the Pb–Pb age of Ibitira, as discussed above. Even more difficult to understand are Sm–Nd model ages of 0.7 Gyr reported by Snyder et al. (1998) for whole rock analyses of two Weekeroo Station inclusions. These are not isochron ages, but rather assume that the initial Sm/Nd elemental ratio up until the dated event was equal to that of chondrites. (Younger Sm–Nd model ages of 3.0 Gyr and 4.27 Gyr were also reported for Watson and Miles, respectively.) No evidence exists in the derived Ar–Ar, I–Xe, and Rb–Sr ages of Weekeroo Station for such a young Sm–Nd model age. Further, Snyder et al. (1998) find old Rb–Sr model ages for the same samples. We have three reasons for suspecting that these young Sm–Nd model ages do not represent significant thermal events on the IIE parent body, but rather are consequences of the model assumptions. First, diffusion of +3 rare earth ions should be slower in comparison to Sr^{+2} and Rb^{+1} ions, and the Sm–Nd chronometer generally is expected to be harder to reset than either the K–Ar or Rb–Sr chronometers (Bogard, 1995). Secondly, if we assume that a single event reset ages in Watson, Netschaëvo, and Kodaikanal (as suggested above), then three radiometric chronometers (K–Ar, Rb–Sr, and Pb–Pb) give essentially the same age, an age significantly older than the Sm–Nd model age of Watson (Table 2). Thirdly, if the young Sm–Nd model ages are real, then each of these three meteorites was affected by a separate thermal event at a very different time, none of which affected other IIE meteorites. If the thermal event that caused resetting of Weekeroo Station's Sm–Nd chronometer also produced differentiation of the silicate, it is difficult to understand why the other chronometers were not also reset. On the other hand, if the thermal event that reset Sm–Nd was a modest one, silicate differentiation for Weekeroo Station must have occurred at an earlier time, and the assumption of a chondritic Sm/Nd ratio before the Sm–Nd model age might not be true.

5. DISCUSSION

5.1. Formation Models for IIE Irons

Any model which attempts to explain the petrology and chronology of IIE irons must explain the basic mechanism by which metal and silicates were mixed to produce the large-scale features observed in IIE meteorites (Fig. 1). Three general classes of models have been proposed. Wasserburg et al. (1968) first suggested that the silicate-bearing IIE Colomera formed through trapping of silicate melts in a small metallic melt pool which was itself enclosed in silicates. These authors rejected a shock origin. The generalized idea that silicate-bearing iron meteorites (e.g., IAB, IIE, and IIICD) and related stony meteorites (e.g., acapulcoites, lodranites, winonaites) formed through partial melting and incomplete differentiation of asteroids which were non-collisionally heated has been widely embraced (see Mittlefehldt et al., 1998 and references therein). In a different model, Wasson and Wang (1986) proposed that IIE iron meteorites formed in individual pools of impact-produced melt in the near-surface region of a chondritic parent body. In the view of Wasson and Wang (1986), melting of the Fe,Ni–FeS and basaltic components and their mixing occurred within these melt pools. This model was invoked by Olsen et al. (1994) to explain the origin of Watson. More recently, Casanova et al. (1995) have called both of these models into question. Casanova et al. (1995) rejected the impact hypothesis of Wasson and Wang (1986) based on the lack of shock features they observed in a single silicate inclusion in Techado. Keil et al. (1997) marshaled evidence against impact as a heat source for any of the silicate-bearing irons or related stones. It is worth noting that the modeling of Keil et al. (1997) suggests that bodies would experience catastrophic fragmentation before significant heating. Such a conclusion may require revision in light of the presence on the intact asteroid Mathilde of numerous craters that are greater than one half the diameter of the asteroid. Casanova et al. (1995) also rejected the model of Wasserburg et al. (1968), because it did not readily explain mixing of chondritic, sometimes angular, inclusions into the metal, such as is seen in Netschaëvo and Techado. Instead, Casanova et al. (1995) invoked a new model in which noncollisional heating produced a range of silicate inclusion types that were collisionally mixed with the metal from the core of another asteroid, akin to models for mesosiderite formation. This hybrid model of noncollisional heating to form basic lithologies, followed by impact mixing to produce the meteorite, would seem capable of generating the broad array of features observed in silicate-bearing IIE irons, although we believe invoking two separate asteroids as sources of these lithologies is unnecessary.

A related question in the case of the IIE irons is whether they originate from the same parent body as the H chondrites. This idea has been suggested by several authors (e.g., Casanova et al., 1995; Olsen et al., 1994) based on similarities in mineral compositions, oxygen isotopic compositions, and some cosmic-ray exposure ages. The association of silicate-bearing IIE irons with the H chondrite parent body has been championed most recently by Gaffey and Gilbert (1998). We point out that several reasons exist to doubt such a link. Mafic silicates in IIE irons exhibit a broad range of compositions from $Fa_{14.1}Fs_{13.8}$ in Netschaevo to $Fs_{23.5}$ in Colomera (e.g., Bunch et al., 1970). In general, the differentiated silicate inclusions are richer in FeO, consistent with enrichment of early partial melts in FeO. However, the most primitive silicate inclusions in IIE irons (Netschaevo, $Fa_{14.1}$; Techado, $Fa_{16.4}$) exhibit olivine compositions outside the range typical for H chondrites ($Fa_{16.9-20.4}$; Gomes and Keil, 1980). We fully recognize, however, that these silicate compositions could have been reduced during

mixing and reaction with the metal. From similarities in oxygen and nitrogen isotopic compositions between H chondrites and IIE irons and between the "young" and "old" IIE irons, Clayton and Mayeda (1996) suggested a link between IIE irons and H chondrites. The mean oxygen isotopic compositions of silicate-bearing IIE irons ($\Delta^{17}O = 0.59 \pm 0.07$; Clayton and Mayeda, 1996) and equilibrated H chondrites ($\Delta^{17}O = 0.73 \pm 0.09$; Clayton et al., 1991) differ by approximately their combined 1σ standard deviation. High-precision oxygen isotopic analyses could possible resolve whether this difference is real. Finally, although the space exposure ages of young IIEs Netschaëvo, Watson, and Kodaikanal are consistent with those of many H chondrites, the exposure ages of Weekeroo Station and Miles are much older than any known H chondrite. We suggest that no convincing evidence exists for a direct link between H chondrites and IIE irons and that these two groups may have originated on different parent asteroids. Though the IIE iron parent body may have originally been broadly "H chondrite-like," it may have differed slightly in mafic silicate and oxygen isotopic compositions, and it appears to have experienced more extensive differentiation than the H chondrite body. This difference in heating may reflect differences in asteroid size, heliocentric distance or timing of formation, although the exact cause remains unknown.

5.2. Chronology Constraints on Formation

The occurrence of both "old" and "young" meteorites within the IIE irons has important implications for their genesis. The compositional trends observed in the metallic portions of these meteorites (Wasson and Wang, 1986) are best explained by their formation on a single parent body. The simplest explanation for their origin would be that a single process produced the silicate/metal assemblages in all IIE irons. However, whereas those IIEs with older ages could have been formed by indigenous metamorphism within the parent body, we do not expect typical asteroids to sustain significant internal heat over times of ~0.8 Gyr. Thus, if the "young" radiometric ages of silicate represent the time of formation of these iron/silicate meteorites, then only impact-induced heating and mixing is a viable model. If noncollisional (i.e., internal) heating early in the history of the parent body produced those meteorites with old ages, then a different mechanism must be invoked to explain the "young" ages. The important chronological issue is whether the young IIE ages must represent formation of the metal/silicate assemblage or, alternatively, age resetting by impact long after these meteorites formed.

The radiometric chronology of silicates in those IIEs with old ages (Table 2) requires that at least some of these metal-silicate assemblages formed and cooled relatively early in solar system history. Further, the differentiated silicate in Sombrerete, which may have originated on a similar, but separate parent body to that of the IIEs, formed within ≤0.02 Gyr of parent body formation. The presence of a low $^{182}W/^{184}W$ ratio in Watson metal also argues for early separation of metal and silicate, before ~4.5 Gyr ago (Snyder et al., 1998). However, variations in radiometric ages also suggest that final chronometer closure of the silicate in some IIE meteorites required a significant time period, as recently as ~4.41 Gyr in the case of the Ar–Ar age of Miles. The initial $^{87}Sr/^{86}Sr$ values also imply a significant difference in Rb–Sr closure times between Colomera and Weekeroo Station. These observations imply formation by an internal thermal process acting over time.

The most striking aspect of the isotopic chronology of IIE silicates is that three meteorites (Netschaëvo, Watson, and Kodaikanal) give relatively young radiometric ages of ~3.68 Gyr. These three also have the youngest space exposure ages and may have been ejected into space from a different part of the parent body. As with essentially all meteorites, there is no evidence that the impact events that initiated space exposure had any significant effect on the radiometric ages of any of the IIEs. It is much harder, however, to correlate petrologic features of IIE silicate with their radiometric age. For example, Netschaëvo, Techado, and Watson all have somewhat primitive, chondritic-like silicates. Netschaëvo compositionally resembles H chondrites and contains angular clasts showing minimum alteration; Techado was obviously heated to significant temperatures, but not differentiated; and Watson was heated sufficiently to segregate metal and sulfide from the silicate. However, the radiometric ages of Netschaëvo and Watson are young, whereas the Ar–Ar age of Techado is ~4.49 Gyr, and certainly not as young as 3.68 Gyr. Silicates in the remaining IIEs show characteristics of being much more differentiated and processed. Whereas three of these more differentiated meteorites give relatively old radiometric ages, Kodaikanal silicate definitely gives a much younger age. The close similarity and likely identity of radiometric ages for Kodaikanal, Netschaëvo, and Watson suggests that these ages were determined by a single process or event operating over a limited period of time, an event that did not affect the other IIEs. The issue is whether that process was the same the process that formed the older IIEs.

Shock reheating may have reset at least the Ar–Ar ages of silicate inclusions in those IIE meteorites with "young" ages. In this work, we have documented extensive shock features in the silicates of some IIEs. The "differentiated" silicate inclusions in Colomera, Weekeroo Station, Miles, Kodaikanal, and Elga all exhibit evidence of extensive postsolidification shock and associated postshock temperature increases of up to ~300°C. Osadchii et al. (1981) has argued that the radiating corona structures observed in these meteorites reflect shock remelting. We agree with this conclusion. Perhaps the most compelling argument for a shock origin for these features is the coexistence over scales of a centimeter of coarse-grained inclusions ± fine-grained, radiating inclusions ± glassy inclusions in meteorites such as Miles and Colomera (Ikeda and Prinz, 1996; Buchwald, 1975; this work). These textures require different cooling rates, which we interpret as a slow, early cooling during formation and a rapid, postshock cooling history. The "primitive" inclusions in Netschaëvo, Techado, and Watson are less shocked, but still exhibit shock features corresponding to postshock temperature increases of ~100 to 150°C. Olsen et al. (1994) documented that shock effects can be extremely heterogeneous. Further, shock effects are often the most severe within the silicate inclusions, probably owing to their different compressibility relative to the metallic host. Thus, it would appear that individual silicate inclusions could have had drastically different shock and thermal histories.

It remains unclear, however, to what extent individual inclusions and isotopic chronometers might have been altered by

shock. Resetting of Ar–Ar ages by impact heating often occurs in meteorites, but Rb–Sr, Pb–Pb, and Sm–Nd ages are not as easily reset (Bogard, 1995; Shih et al., 1994). Impact heating may have been sufficient to reset Pb–Pb and Rb–Sr in Kodaikanal, which is the most extensively shocked of the silicate-bearing IIE irons. However, Burnett and Wasserburg (1967a) concluded that the Rb–Sr system in Kodaikanal could not have been reset at ~3.7 Gyr by simple homogenization of Sr isotopes, but rather that chemical fractionation and physical separation must have occurred near this time. The initial $^{87}Sr/^{86}Sr$ ratio at the time of the dated event was not well defined. Even so, Kodaikanal Rb/Sr could have evolved between ~4.5 and ~3.7 Gyr ago in a chondrite-like system, but it could not have evolved over this time period with the Rb/Sr ratio measured in one of the inclusions (Burnett and Wasserburg, 1967a). It is not clear if impact heating could produce the differentiation and material interchange among different silicate inclusions within Kodaikanal that these data would require (e.g., Keil et al., 1997). It also is not clear that such metal–silicate mixing could occur without remelting both silicate and metal. If melting, differentiation, and chemical fractionation did occur during an impact event 3.68 Gyr ago, this event would represent the formation of Kodaikanal, and would violate any simple assumption that all IIE meteorites were formed by the same early process.

The Rb–Sr, Sm–Nd, and Pb–Pb systematics, including the $^{87}Sr/^{86}Sr$ and $^{143}Nd/^{144}Nd$ initial ratios, for the "primitive" inclusions in Netschaëvo and Watson have not been determined, so we do not know if these chronometers also indicate a young age for these meteorites. The primitive and undifferentiated nature of Netschaëvo silicate requires that it formed early. This characteristic suggests that radiometric ages other than Ar–Ar may not have been extensively reset. On the other hand, Netschaëvo did not give an ^{129}I–^{129}Xe correlation (Niemeyer, 1980). A single Rb–Sr analysis of Watson silicate (Snyder et al., 1998) plots close to the array defined by the Weekeroo Station Rb–Sr data (Burnett and Wasserburg, 1967b). However, this does not rule out impact resetting of Rb–Sr. In addition, the isotopic composition of tungsten in Watson metal and silicate are not the same (Snyder et al., 1998), indicating that the metal and silicate were not in isotopic equilibrium after the decay of ^{182}Hf ($T½ = 9$ Myr). The $^{182}W/^{184}W$ ratio in Watson metal has a small negative anomaly, similar to that of other iron meteorites, but this ratio in Watson silicate does not show the higher anomaly found in some differentiated stony meteorites. Snyder et al. (1998) suggest that this difference is evidence that Watson metal and silicate derived from separate parent bodies. However, the data might also be explained if Watson silicate was not separated from metal until after ^{182}Hf decayed, and the silicate was later mixed with other metal that last equilibrated with silicate before ^{182}Hf decay.

6. CONCLUSIONS

We suggest that silicate differentiation and mixing with metal to form those IIE meteorites with highly differentiated silicates can be explained by variable degrees of metamorphism and melting caused by indigenous heat produced within an H chondrite-like parent body shortly after its formation. In such a process, an Fe,Ni–FeS melt forms first between 950 and 1000°C, followed by a feldspar-enriched basaltic-like melt at temperatures in excess of 1050°C. Migration of these melts due to thermal gradients deep within the parent body could produce a mixture of metal and basaltic silicates, leaving ultramafic olivine-pyroxene rocks as residues. Clearly, a broad range of differentiation occurred throughout the IIE parent body. Differentiation proceeded to a significant degree in some parts of the body and resulted in large masses of metal and highly differentiated silicate, whereas silicate in other parts of the body was unaltered. The tendency for silicate in the more differentiated IIEs (and in Sombrerete) to consist of small globular inclusions suggests that these silicates were plastic or molten when mixed with metal, which probably also was molten. This seems consistent with formation of these more differentiated meteorites in parts of the body which were hotter and experienced higher degrees of silicate differentiation. This differentiation and mixing of metal and silicate in IIEs with older ages must have occurred relatively soon after the parent body formed. The apparent range in ages among some differentiated IIEs may have been produced either by an extended period in which differentiation of the silicate and mixing of this silicate with metal occurred, or by relatively slow cooling after this mixing.

Our preferred formation mechanism described above for those IIEs with highly differentiated silicates also may have occurred on some other parent bodies. Certainly, the petrographic and chronologic similarities between IIEs with globular inclusions and Sombrerete inclusions strongly suggests that the same process operating on the IIE parent body operated on the parent asteroid of Sombrerete. Unfortunately, Sombrerete appears to be our only sample of this asteroid. A similar process has been inferred to explain the coexistence of metal with both mafic and basaltic silicate in the Caddo County IAB iron meteorite (Takeda et al., 2000). An analogous process may have formed primitive achondrites like winonaites and lodranites, which are believed to have been derived by partial melting and varying degrees of silicate and metal differentiation within parent bodies resembling H chondrites (McCoy et al., 1997; Benedix et al., 1998). The parent bodies of winonaites and IAB irons may have been the same (Benedix et al., 1998).

Available data do not uniquely define a specific model for the origin of those IIE meteorites with undifferentiated silicate. In principle, two different explanations are possible. The first is that the metal–silicate mixture for all IIEs formed early, and the young radiometric ages for Netschaëvo, Watson and Kodaikanal were reset by impact heating long after formation. The second explanation is that the metal–silicate mixing of the young IIEs occurred 3.68 Gyr ago, and of necessity was caused by large–scale impact. An issue relating to this second explanation is whether the metal would have to be melted and the silicate differentiated at the time of formation, or whether the mixing could be accomplished in the solid state. Existence of still-primitive silicate within Netschaëvo and Techado demonstrates that silicate–metal mixing occurred in these meteorites without causing appreciable differentiation of the silicate. Presumably at the time of mixing, these silicates were relatively cold and the metal relatively hot, and the mixed assemblage cooled quickly. This suggests that silicate in these two meteorites originated from a much cooler region of the parent body,

in comparison to the more differentiated IIEs, including Kodaikanal. Residual heat from the hot metal may have produced the recrystallized texture observed in the small Techado silicate inclusion described by Casanova et al. (1995). These characteristics suggest impact as the mixing process for formation of Techado and Netschaëvo.

No measured characteristic of Netschaëvo and Watson seems to require that the silicate/metal assemblage of these two meteorites formed significantly later than ~4.5 Gyr ago. The silicate and metal could have derived from the same parent body and could have been brought into association by a large impact ~4.5 Gyr ago that excavated deeply. The reset Ar–Ar ages of Netschaëvo and Watson may have been produced by moderate shock heating at 3.68 Gyr, long after the silicate–metal mixtures formed. The unaltered nature of the silicate in Netschaëvo indicates that the impact event did not produce silicate melting and may not have reset the Rb–Sr and Sm–Nd chronometers. (It would be informative to determine Rb–Sr and Sm–Nd isochron ages of Netschaëvo and Watson silicate, to see if any significant evidence of resetting exists. Such a study should also include petrography to document the possible effects of shock reheating.) In a similar model, Casanova et al. (1995) concluded that impact mixing involved silicates from one parent body with a metal core from a different parent body.

Formation of Kodaikanal presents the greatest challenge in explaining the origin and chronology of IIEs. The close similarity in radiometric ages among Kodaikanal, Netschaëvo, and Watson suggests resetting by the same impact event. However, both extensive resetting of radiometric ages and silicate fractionation obviously occurred in Kodaikanal, and it is not obvious that these changes could have been accomplished without appreciable melting of both silicate and metal 3.68 Gyr ago. Thus, separate mechanisms may have produced the differentiated silicate in Kodaikanal compared to other strongly differentiated IIEs. In spite of arguments that have been presented against impact-produced differentiation (Keil et al., 1997), we may have to reevaluate the ability of a large impact to produce widespread melting and differentiation in meteorites. If this is indeed the case, the situation may exist that similar mixtures of strongly differentiated silicate and metal were produced in the same parent body at different times by completely different mechanisms. The 3.68 Gyr age of this impact event falls within a period of time when the moon was being impacted with large objects producing major basins and when the parent body of eucrites (Vesta?) was also experiencing impacts of sufficient size to reset Ar–Ar ages (Bogard, 1995).

Acknowledgments—We thank A. Brearley (Univ. of New Mexico), K. Keil (Univ. of Hawaii), R. S. Clarke, Jr., and G. J. MacPherson (Smithsonian Institution), G. J. Wasserburg (California Institute of Technology) and J. Shwade for kindly providing samples for this study. Expert technical assistance from V. Yang and T. Servilla is appreciated. This manuscript has benefited substantially from helpful discussions with I. Casanova, and from detailed reviews by T. Swindle, E. Olsen, and an anonymous reviewer.

This work was supported by NASA Grant NAG 5-4490 (TJM) and RTOP 344-31-30-05 (DDB).

REFERENCES

Alexander E. C. and Davis P. K. (1974) ^{40}Ar–^{39}Ar ages and trace element contents of Apollo 14 breccias: An interlaboratory cross-calibration of ^{40}Ar–^{39}Ar standards. *Geochim. Cosmochim. Acta* **38,** 911–928.

Bence A. E. and Burnett B. S. (1969) Chemistry and mineralogy of the silicates and metal of the Kodaikanal meteorite. *Geochim. Cosmochim. Acta* **33,** 387–407.

Benedix G. K., McCoy T. J., Keil K., Bogard D. D., and Garrison D. H. (1998) A petrologic and isotopic study of winonaites: Evidence for early partial melting, brecciation, and metamorphism. *Geochim. Cosmochim. Acta* **62,** 2535–2553.

Bevington P. R. (1969) *Data Reduction and Error Analysis for the Physical Sciences*. McGraw-Hill.

Bild R. W. and Wasson J. T. (1977) Netschaëvo: A new class of chondritic meteorite. *Science* **197,** 58–62.

Birck J. L. and Allègre C. J. (1978) Chronology and chemical history of the parent body of basaltic achondrites studied by the ^{87}Rb/^{87}Sr method. *Earth Planet. Sci. Lett.* **39,** 37–51.

Birck J. L. and Allègre C. J. (1998) ^{187}Re–^{187}Os in iron meteorites and the strange origin of the Kodaikanal meteorite. *Meteorit. Planet. Sci.* **33,** 647–653.

Bogard D. D. (1995) Impact ages of meteorites: A synthesis. *Meteoritics* **30,** 244–268.

Bogard D. D. and Cressy P. J. (1973) The production rates of ^{3}He, ^{21}Ne, and ^{38}Ar from target elements in the Bruderheim chondrite. *Geochim. Cosmochim. Acta* **37,** 527–546.

Bogard D. D. and Garrison D. H. (1998) ^{39}Ar–^{40}Ar ages and thermal history of mesosiderites. *Geochim. Cosmochim. Acta* **62,** 1459–1468.

Bogard D. D. and Garrison D. H. (1999) ^{39}Ar–^{40}Ar dating of thermal events on meteorite parent bodies. *Lunar Planet. Sci.* **XXX,** 1104.

Bogard D. D., Burnett D. S., Eberhardt P., and Wasserburg G. J. (1968) ^{40}Ar–^{40}K ages of silicate inclusions in iron meteorites. *Earth Planet. Sci. Lett.* **3,** 275–283.

Bogard D. D., Burnett D. S., and Wasserburg G. J. (1969) Cosmogenic rare gases and the ^{40}K–^{40}Ar age of the Kodaikanal iron meteorite. *Earth Planet. Sci. Lett.* **5,** 273–281.

Bogard D. D., Huneke J. C., Burnett D. S., and Wasserburg G. J. (1971a) Xe and Kr analyses of silicate inclusions from iron meteorites. *Geochim. Cosmochim. Acta* **35,** 1231–1254.

Bogard D. D., Funkhouser J. G., Schaeffer O. A., and J. Zähringer. (1971b) Noble gas abundances in lunar material - cosmic-ray spallation products and radiation ages from the Sea of Tranquility and the Ocean of Storms. *J. Geophys. Res.* **76,** 2757–2779.

Bogard D. D., Garrison D. H., Norman M., Scott E. R. D., and Keil K. (1995) ^{39}Ar–^{40}Ar age and petrology of Chico: Large-scale impact melting on the L-chondrite parent body. *Geochim. Cosmochim. Acta* **59,** 1383–1399.

Brazzle R. H., Pravdivtseva O. V., Meshik A. P., and Hohenberg C. M. (1999) Verification and interpretation of the I–Xe chronometer. *Geochim. Cosmochim. Acta* **63,** 739–760.

Buchwald V. F. (1975) *Handbook of Iron Meteorites.* Univ. California Press.

Bunch T. E. and Olsen E. (1968) Potassium feldspar in Weekeroo Station, Kodaikanal, and Colomera iron meteorites. *Science* **160,** 1223–1225.

Bunch T. E., Keil K. and Olsen E. (1970) Mineralogy and petrology of silicate inclusions in iron meteorites. *Contrib. Min. Petrol.* **25,** 297–240.

Burnett D. S. and Wasserburg G. J. (1967a) Evidence for the formation of an iron meteorite at 3.8 × 109 years. *Earth Planet. Sci. Lett.* **2,** 137–147.

Burnett D. S. and Wasserburg G. J. (1967b) ^{87}Rb–^{87}Sr ages of silicate inclusions in iron meteorites. *Earth Planet Sci. Lett.* **2,** 397–408.

Casanova I., Graf T., and Marti K. (1995) Discovery of an unmelted H-chondrite inclusion in an iron meteorite. *Science* **268,** 540–542.

Chen J. H. and Wasserburg G. J. (1985) U–Th–Pb isotopic studies on meteorite ALHA81005 and Ibitira. *Lunar Planet. Sci.* **XVI,** 119–120.

Clayton R. N., Mayeda T. K., Goswami J. N., and Olsen E. J. (1991) Oxygen isotope studies of ordinary chondrites. *Geochim. Cosmochim. Acta* **55,** 2317–2337.

Clayton R. N. and Mayeda T. K. (1996) Oxygen isotope studies of achondrites. *Geochim. Cosmochim. Acta* **60,** 1999–2017.

Evensen N. M., Hamilton P. J., Harlow G. E., Klimentidis R., O'Nions

R. K., and Prinz M. (1979) Silicate inclusions in Weekeroo Station: Planetary differentiates in an iron meteorite. *LPSC* **X,** 376–378 (abstr.).

Eugster O. and Michel T. (1995) Common asteroid break-up events of eucrites, diogenites, and howardites and cosmic-ray production rates for noble gases in achondrites. *Geochim. Cosmochim. Acta* **59,** 177–199.

Eugster O. (1988) Cosmic-ray production rates for ^{3}He, ^{21}Ne, ^{38}Ar, ^{83}Kr, and ^{126}Xe in chondrites based on ^{81}Kr–Kr exposure ages. *Geochim. Cosmochim. Acta* **52,** 1649–1662.

Freundel M., Schultz L., and Reedy R. C. (1986) Terrestrial ^{81}Kr–Kr ages of Antarctic meteorites. *Geochim. Cosmochim. Acta* **50,** 2663–2673.

Gaffey M. J. and Gilbert S. L. (1998) Asteroid 6 Hebe: The probable parent body of the H-type ordinary chondrites and the IIE iron meteorites. *Meteorit. Planet. Sci.* **33,** 1281–1295.

Garrison D. H. and Bogard D. D. (1998) Isotopic composition of trapped and cosmogenic noble gases in several Martian meteorites. *Meteorit. Planet. Sci.* **33,** 721–736.

Garrison D. H., Bogard D. D., Albrecht A. A., Vogt S., Herzog G. F., Klein J., Fink D., Dezfouly–Arjomandy B., and Middleton R. (1992) Cosmogenic nuclides in core samples of the Chico L6 chondrite: Evidence for irradiation under high shielding. *Meteoritics* **27,** 371–381.

Gomes C. B. and Keil K. (1980) *Brazilian Stone Meteorites.* Univ. New Mexico Press.

Göpel C., Manhès G., and Allègre C. J. (1985) Concordant 3,676 Myr U–Pb formation age for the Kodaikanal iron meteorite. *Nature* **317,** 341–344.

Graf T. and Marti K. (1995) Collisional history of H chondrites. *J. Geophys. Res.* **100,** 21247–21263.

Graf T., Baur H., and Signer P. (1990) A model for the production of cosmogenic nuclides in chondrites. *Geochim. Cosmochim. Acta* **54,** 2521–2534.

Herpfer M. A., Larimer J. W., and Goldstein J. I. (1994) A comparison of metallographic cooling rate methods used in meteorites. *Geochim. Cosmochim. Acta* **58,** 1353–1366.

Hohenberg C. M., Marti K., Podosek F. A., Reedy R. C., and Shirck J. R. (1978) Comparisons between observed and predicted cosmogenic noble gases in lunar samples. *Proc. Lunar Planet. Sci. Conf.* **9,** 2311–2344.

Hohenberg C. M., Hudson B., Kennedy B. M., and Podosek F. A. (1981) Noble gas retention chronologies for the St. Sèverin meteorite. *Geochim. Cosmochim. Acta* **45,** 535–546.

Ikeda Y. and Prinz M. (1996) Petrology of silicate inclusions in the Miles IIE iron. *Proc. NIPR Symp. Antarct. Meteorites* **9,** 143–173.

Ikeda Y., Yamamoto T., Kojima H., Imae N., Kong P., Ebihara M., and Prinz M. (1997a) Yamato-791093, a metal–sulfide-enriched H-group chondritic meteorite transitional to primitive IIE irons with silicate inclusions. *Antarct. Meteorite Res.* **10,** 335–353.

Ikeda Y., Ebihara M., and Prinz M. (1997b) Petrology and chemistry of the Miles IIE iron. I: Description and petrology of twenty new silicate inclusions. *Antarctic. Meteorite Res.* **10,** 355–372.

Jentsch O. and Schultz L. (1996) Cosmogenic noble gases in silicate inclusions of iron meteorites: Effects of bulk composition on elemental production rates. *J. Royal Soc. West. Australia* **79,** 67–71.

Keil K., Stöffler D., Love S. G., and Scott E. R. D. (1997) Constraints on the role of impact heating and melting in asteroids. *Meteoritics Planet. Sci.* **32,** 349–363.

Malvin D. J., Wang D., and Wasson J. T. (1984) Chemical classification of iron meteorites –X. Multielement studies of 43 irons, resolution of group IIIE from IIIAB, and evaluation of Cu as a taxonomic parameter. *Geochim. Cosmochim. Acta* **48,** 785–804.

Manhes G., Göpel C., and Allègre C. J. (1987) High resolution chronology of the early solar system based on lead isotopes. *Meteoritrics* **22**, 453–454 (abstr.).

Marti K., Eberhardt P., and Geiss J. (1966) Spallation, fission, and neutron capture anomalies in meteoritic krypton and xenon. *Z. Naturforsch* **21a,** 388–413.

McCoy T. J., Keil K., Clayton R. N., Mayeda T. K., Bogard D. D., Garrison D. H., Huss G. R., Hutcheon I. D., and Wieler R. (1996) A petrologic, chemical and isotopic study of Monument Draw and comparison with other acapulcoites: Evidence for formation by incipient partial melting. *Geochim. Cosmochim. Acta* **60,** 2681–2708.

McCoy T. J., Keil K., Clayton R. N., Mayeda T. K., Bogard D. D., Garrison D. H., and Wieler R. (1997) A petrologic and isotopic study of lodranites: Evidence for early formation as partial melt residues from heterogeneous precursors. *Geochim. Cosmochim. Acta* **61,** 623–637.

Minster J. F., Birck J. L., and Allègre C. J. (1982) Absolute age of formation of chondrites studied by the ^{87}Rb–^{87}Sr method. *Nature* **300,** 414–419.

Mittlefehldt D. W., Lindstrom M. M., Bogard D. D., Garrison D. H., and Field S. W. (1996) Acapulco- and Lodran-like achondrites: Petrology, geochemistry, chronology and origin. *Geochim. Cosmochim. Acta* **60,** 867–882.

Mittlefehldt D. W., McCoy T. J., Goodrich C. A., and Kracher A. (1998) Non-chondritic meteorites from asteroidal bodies. In *Planetary Materials* (J. J. Papike, ed.), Chapter 4, pp. 4-1-4-195. *Rev. Mineral.* **36**.

Niemeyer S. (1979) ^{40}Ar–^{39}Ar dating of inclusions from IAB iron meteorites. *Geochim. Cosmochim. Acta* **43,** 1829–1840.

Niemeyer S. (1980) I–Xe and ^{40}Ar–^{39}Ar dating of silicate from Weekeroo Station and Netschaëvo IIE iron meteorites. *Geochim. Cosmochim. Acta* **44,** 33–44.

Olsen E. and Jarosewich E. (1970) The chemical composition of the silicate inclusions in the Weekeroo Station iron meteorite. *Earth Planet. Sci. Lett.* **8,** 261–266.

Olsen E. and Jarosewich E. (1971) Chondrules: First occurrence in an iron meteorite. *Science* **174,** 583–585.

Olsen E., Davis A., Clarke R. S. Jr, Schultz L., Weber H. W., Clayton R., Mayeda T., Jarosewich E., Sylvester P., Grossman L., Wang M.-S., Lipschutz M. E., Steele I. M., and Schwade J. (1994) Watson: A new link in the IIE iron chain. *Meteoritics* **29,** 200–213.

Osadchii Eu. G., Baryshnikova G. V., and Novikov G. V. (1981) The Elga meteorite: Silicate inclusions and shock metamorphism. *Proc. Lunar Planet. Sci. Conf.* **12B,** 1049–1068.

Onstott T. C., Miller M. L., Ewing R. C., Arnold G. W., and Walsh D. S. (1995) Recoil refinements: implications for the ^{40}Ar/^{39}Ar dating technique. *Geochim. Cosmochim. Acta* **59,** 1821–1834.

Pepin R. O. (1991) On the origin and early evolution of terrestrial planet atmospheres and meteoritic volatiles. *Icarus* **92,** 2–79.

Prinz M., Nehru C. E., and Delaney J. S. (1982) Sombrerete: An iron with highly fractionated amphibole-bearing Na–P-rich silicate inclusions. *Lunar Planet. Sci.* **XIII,** 634–635.

Prinz M., Nehru C. E., Delaney J. S., Weisberg M., and Olsen E. (1983) Globular silicate inclusions in IIE irons and Sombrerete: Highly fractionated minimum melts. *LPSC* **XIV,** 618–619.

Rubin A. E., Jerde E. A., Zong P., Wasson J. T., Westcott J. W., Mayeda T. K., and Clayton R. N. (1985) Properties of the Guin ungrouped iron meteorite: The origin of Guin and of group-IIE irons. *Earth Planet. Sci. Lett.* **76,** 209–226.

Rubin A. E. and Ulff–Moller F. (1999) The Portales Valley meteorite breccia: Evidence for impact-induced metamorphism of an ordinary chondrite. *LPSC* **XXX,** 1125 (abstr.).

Sanz H. G., Burnett D. S., and Wasserburg G. J. (1970) A precise ^{87}Rb/^{87}Sr age and initial ^{87}Sr/^{86}Sr for the Colomera iron meteorite. *Geochim. Cosmochim. Acta* **34,** 1227–1239.

Schultz L. and Freundel M. (1985) On the production rate of ^{21}Ne in ordinary chondrites. In *Isotopic Ratios in the Solar System* (ed. Centre National d-etudes spatiales), pp. 27–33, Cepadues-Editions, Toulouse.

Shih C. Y., Nyquist L. E., Bogard D. D., and Wiesmann H. (1994) K–Ca and Rb–Sr dating of two lunar granites: Relative chronometer resetting. *Geochim. Cosmochim. Acta* **58,** 3101–3116.

Signer P. and Nier A. O. (1960) The distribution of cosmic-ray-produced rare gases in iron meteorites. *J. Geophys. Res.* **65,** 2947–2964.

Snyder G. A., Lee D. C., Ruzicka A. M., Taylor L. A., Halliday A. N., and Prinz M. (1998) Evidence of late impact fractionation and mixing of silicates on iron meteorite parent bodies: Hf–W, Sm–Nd, and Rb–Sr isotopic studies of silicate inclusions in IIE irons. *LPSC* **XXIX,** 1142 (abstr.).

Steiger R. And Jäger E. (1977) Subcommission on geochronology:

Convention on the use of decay constants in geo- and cosmochronology. *Earth Planet. Sci. Lett.* **36,** 359–362.
Stöffler D., Keil K., and Scott E. R. D. (1991) Shock metamorphism of ordinary chondrites. *Geochim. Cosmochim. Acta* **55,** 3845–3867.
Takeda H., Bogard D. D., Mittlefehldt D. W., and Garrison D. H. (2000) Mineralogy, petrology, chemistry, and ^{39}Ar–^{40}Ar and exposure ages of the Caddo County IAB iron: Evidence for early partial melt segregation of a gabbro area rich in plagioclase-diopside. *Geochim. Cosmochim. Acta*, 1311–1327.
Treiloff M., Jessberger E. K., and Oehm J. (1989) Ar–Ar ages of LL chondrites. *Meteoritics* **24,** 332 (abstr.).
Wasserburg G. J., Sanz H. G., and Bence A. E. (1968) Potassium–feldspar phenocrysts in the surface of Colomera, an iron meteorite. *Science* **161,** 684–687.
Wasson J. T. and Wang J. (1986) A nonmagmatic origin of group-IIE iron meteorites. *Geochim. Cosmochim. Acta* **50,** 725–732.

APPENDIX 1

Ar isotopic data, K/Ca ratios, and Ar–Ar ages (in Gyr) for irradiated samples (Table A-1). Isotopic ratios have been multiplied by the factors indicated. Uncertainties are shown beneath each value. Also shown for each sample are the irradiation constant (*J* value) and its uncertainty. Age uncertainties include only the error in $^{40}Ar/^{39}Ar$ and not the error in *J*.

APPENDIX 2

Derivation of Cosmogenic Production Rates and Exposure Ages for IIEs

Silicates from IIEs show a rather wide variation in mineralogy and composition (Mittlefehldt et al., 1998). As discussed earlier, Netschaëvo and Techado silicates are less differentiated and have compositions similar to those of H chondrites (Bunch et al., 1970; Olsen and Jarosewich, 1971; Bild and Wasson, 1977; Casanova et al.,1995). Eugster (1988) determined the absolute ^{21}Ne and ^{38}Ar production rates for H chondrites by using the relative chemical element factors reported by Schultz and Freundel (1985) and Freundel et al. (1986) and then normalizing these rates to ^{81}Kr–Kr exposure ages for several chondrites. The ^{38}Ar production rates for chondrites was later revised downward by ~11% (Graf and Marti, 1995). We used these H-chondrite production rates to calculate the Netschaëvo ages in Table 4. In a second method of determining absolute production rates, Eugster and Michel (1995) used similar chemical production factors as did Schultz and Freundel (1985), but normalized the cosmogenic ^{3}He, ^{21}Ne, ^{38}Ar, and ^{81}Kr–Kr data separately for suites of eucrites and diogenites. This method gives the option of calculating production rates as a function of the chemical composition. Applying this method to the Netschaëvo data gives essentially the same exposure ages as those calculated from H-chondrite production rates. We attribute the lower ^{3}He age compared to the ^{21}Ne and ^{38}Ar ages to diffusive loss of ^{3}He. Netschaëvo was apparently forged, which would certainly contribute to He loss, and the ^{4}He concentration of Netschaëvo appears low as well (Table 3). Some ^{21}Ne may have been lost. We suggest that the higher ^{38}Ar age of 18 Ma that Niemeyer, (1980) reported for an irradiated sample of Netschaëvo may have been caused by ^{38}Ar produced from neutron capture on ^{37}Cl in the reactor, a possibility also mentioned by the author.

Silicates from Watson, Miles, and Sombrerete may originally have had a composition similar to H-chondrites, but they have lost most of their metal and sulfur. Absence of chondritic metal not only lowers the Fe concentration but also increases the concentration of other target elements producing cosmogenic Ne and Ar (e.g., Mg, Si, and Ca) relative to the composition of chondrites. For Miles and Sombrerete we used the chemical compositions reported by Ikeda and Prinz (1996) and Prinz et al. (1982), respectively. We used the production rate equations of Eugster and Michel (1995) for eucrites as opposed to that for diogenites (the latter would be ~8% lower for ^{21}Ne). For ^{21}Ne production we added in an additional factor for Na (Hohenberg et al., 1978), which exists in considerably greater abundance than in eucrites. The Ca concentrations determined for our irradiated samples of Miles and Sombrerete were considerably lower than those reported by Ikeda and Prinz (1996) and Prinz et al. (1982). Consequently, we give two values for the ^{38}Ar ages for Miles and Sombrerete (Table 4). The first entry assumes the literature Ca values, and the second entry assumes the Ca values we determined on irradiated samples. The ^{3}He and ^{21}Ne ages are essentially the same for either Ca value. The much closer agreement between ^{21}Ne and ^{38}Ar ages for Miles using our determined Ca (~218 Ma) suggests that this value is more appropriate. For Sombrerete, the ^{38}Ar ages are much higher compared to the ^{3}He and ^{21}Ne ages by using either Ca abundance. The Sombrerete ^{38}Ar abundance is unlikely to be in error, because similar cosmogenic ^{38}Ar and radiogenic ^{40}Ar concentrations were measured for the neutron-irradiated sample. Only if we assume the Ca concentration in our unirradiated sample was ~12%, or considerably larger than that we measured in the irradiated sample or that reported by Prinz et al. (1982), would the ^{21}Ne and ^{38}Ar ages for Sombrerete become concordant. Alternatively, Sombrerete may have lost both ^{3}He and ^{21}Ne by diffusion. Thus, we consider the ^{21}Ne age for Sombrerete to be a lower limit for its space exposure time.

To calculate ages for Colomera, we used the production equations of Eugster and Michel (1995) and Al and Si abundances reported for Colomera feldspar by Bunch and Olsen (1968). Our irradiated sample gave [Ca] = 3.39% and [K] = 13.0%. This K is almost as large as the pure orthoclase concentration of 14% and indicates that Mg and Fe are essentially absent. The relative elemental factors for calculating ^{38}Ar production rates originally used K/Ca = 7 derived from mineral separates of the Bruderheim chondrite (Bogard and Cressy, 1973; Freundel et al., 1986). However, Eugster and Michel (1995) adopted K/Ca =1.6, based on data from 1.6 GeV proton irradiation of a silicate target. The very large K in Colomera feldspar presents an opportunity to compare the two different K/Ca production ratios for ^{38}Ar. By using K/Ca = 1.6 in the method of Eugster and Michel (1995) gives for Colomera feldspar an ^{38}Ar age of 103 Myr and a ^{21}Ne age of 35 Myr. The low ^{3}He age indicates diffusive loss, as might be expected for He in feldspar. Use of K/Ca = 7 in the production equation gives an ^{38}Ar age of 27 Myr by using the chemical equations of Eugster and Michel (1995) and 31 My by using the equations of Schultz and Freundel (1985). Thus, the use of K/Ca = 7 in the production equation gives much better agreement between ^{38}Ar and ^{21}Ne ages than the 1.6 ratio used by Eugster and Michel (1995). This comparison suggests that the higher K/Ca production ratio is preferable. (The ^{38}Ar ages for Sombrerete in Table 4 also were calculated by using a K/Ca production ratio of 7; the ^{38}Ar ages calculated by using a ratio of 1.6 would be considerably larger.)

The Watson exposure ages given in Table 4 are from Olsen et al. (1994) and apparently were calculated by using the method of Eugster and Michel (1995) and the chemical composition determined in that study. The Techado silicate exposure ages were calculated from two analyses reported by Casanova et al. (1995) by using the H-chondrite production rates of Eugster (1988). The ^{38}Ar age calculated from our irradiated sample would be ~45 Ma (assuming all ^{38}Ar is cosmogenic). The ^{38}Ar age for Techado metal was calculated by Casanova et al. (1995) and used production rates derived from ^{40}K and ^{36}Cl. The space exposure ages listed for Kodaikanal and Weekeroo Station are calculated from cosmogenic noble gases in the metal phase. Cosmogenic noble gas ratios for Kodaikanal metal indicate irradiation near the meteoroid surface (e.g., Signer and Nier, 1960) and probably give a reliable exposure age of 12 to 15 Myr (Bogard et al., 1969). However, cosmogenic noble gas ratios for Weekeroo Station metal are not well behaved, and the production rates are more uncertain. We used the Weekeroo Station metal noble gas concentrations and the Kodaikanal metal production rates given by Bogard et al. (1969) to calculate the Weekeroo Station exposure age in Table 4. Significantly greater shielding compared to Kodaikanal would make these Weekeroo Station ages even older. Niemeyer (1980) reported ^{38}Ar and ^{126}Xe ages for Weekeroo Station silicate of 350 to 930 Ma.

APPENDIX 3

Detailed Comparison of Ar–Ar ages of Watson and Netschaëvo

Because the Ar–Ar ages for Watson and Netschaëvo were determined using different age monitors, we must consider the relative reliability of these monitors to assess whether the small difference in derived meteorite ages is real. The NL-25 hornblende irradiated

with Watson has a totally flat Ar–Ar release spectrum, and its age of 2.65 Gyr is believed known to ±0.5% (Bogard et al., 1995). St. Severin would appear to be a less accurate irradiation standard. The absolute ^{129}I–^{129}Xe age of St. Severin feldspar was determined to be 4.558 Gyr (Brazzle et al., 1999). The K–Ar age of Saint Severin was assumed to be 4.425 ± 0.019 Gyr by Niemeyer (1979; 1980), and his reported age for Netschaëvo was 3.79 ± 0.03 Gyr. However, later Ar–Ar analyses of four St. Severin samples by Hohenberg et al. (1981) and Treiloff et al. (1989) gave limited "plateau" ages of 4.42, 4.38, 4.35, and 4.34 Gyr. In their consideration of Niemeyer's data, Herpfer et al. (1994) adopted a St. Severin age of 4.373 ± 0.030 Gyr, the average of these four new analyses. This is the St. Severin age we used to correct the Netschaëvo and Weekeroo Station Ar–Ar ages reported in Table 2. However, the apparent Ar–Ar ages for St. Severin are not constant with extraction temperature, making a precise determination of the St. Severin age both difficult and dependent on the temperature range utilized. In their original calibration of St. Severin as an irradiation age monitor, Alexander and Davis (1974) used a single extraction of 800 to 1600°C. Niemeyer (1979) based his determination of the irradiation constant on several 900 to 1450°C extractions of St. Severin, but did not report his St. Severin data. In the two St. Severin analyses reported by Hohenberg et al. (1981), this temperature range yields Ar–Ar ages showing a broad spread of 4.21 to 4.45 Gyr, and the Ar–Ar ages spread over 0.4 Gyr for all of the St. Severin extractions. Further, because St. Severin experienced parent body metamorphism, its ^{39}Ar–^{40}Ar age probably cannot be directly compared with ages of chondrites determined by other radiometric techniques, as was originally done by Alexander and Davis (1974). We conclude, therefore, that the variability in the Ar–Ar age of the St. Severin irradiation monitor is sufficiently great such that the uncertainty in the 3.74_5 Gyr Ar–Ar age of Netschaëvo likely overlaps the 3.676 Gyr Ar–Ar age for Watson.

Table A-1. Ar isotopic data for irradiated samples.

Temp. C	39Ar ccSTP/g × e+8	AGE Gyr ±	K/Ca ×100 ±	40/39 ×1 ±	38/39 ×100 ±	37/39 ×100 ±	36/39 ×1000 ±
Watson		47.2 mg J = 0.980 ± 0.0002					
400	2.628	2.677	27.04	34.31	189.39	203.41	5.48
		0.008	0.31	0.20	1.55	2.36	0.80
450	1.234	3.843	64.11	74.62	32.93	85.78	0.22
		0.004	0.67	0.18	0.21	0.89	0.24
500	1.744	3.968	74.17	80.69	12.95	74.15	0.05
		0.002	0.75	0.12	0.16	0.75	0.22
550	3.137	3.909	87.14	77.80	4.39	63.12	0.27
		0.002	0.88	0.08	0.13	0.64	0.15
600	5.573	3.791	166.39	72.22	1.69	33.05	0.15
		0.001	1.67	0.06	0.13	0.33	0.09
625	5.739	3.729	234.72	69.43	1.04	23.43	0.14
		0.001	2.37	0.05	0.13	0.24	0.09
650	9.551	3.685	227.40	67.54	1.20	24.19	0.21
		0.001	2.29	0.05	0.13	0.24	0.08
675	5.744	3.670	272.05	66.89	0.67	20.22	0.01
		0.001	2.75	0.05	0.13	0.20	0.06
725	10.132	3.672	235.60	66.97	0.73	23.34	0.03
		0.001	2.36	0.03	0.13	0.23	0.06
750	12.281	3.678	240.94	67.23	0.49	22.83	0.02
		0.002	2.43	0.07	0.13	0.23	0.05
775	10.902	3.682	248.87	67.42	0.32	22.10	0.15
		0.001	2.50	0.06	0.13	0.22	0.07
800	10.607	3.681	221.68	67.34	0.29	24.81	0.36
		0.001	2.23	0.06	0.13	0.25	0.10
825	9.557	3.675	200.73	67.09	0.28	27.40	0.02
		0.001	2.01	0.04	0.13	0.27	0.06
875	8.423	3.675	157.87	67.08	0.35	34.84	0.25
		0.001	1.59	0.06	0.13	0.35	0.10
910	5.770	3.667	92.42	66.77	0.60	59.51	0.03
		0.001	0.93	0.04	0.13	0.60	0.08
950	5.284	3.644	64.89	65.78	0.95	84.75	0.87
		0.002	0.65	0.06	0.13	0.85	0.14
1000	5.567	3.632	39.95	65.30	1.05	137.69	0.66
		0.002	0.40	0.06	0.13	1.38	0.21
1075	9.331	3.627	23.77	65.09	0.94	231.35	0.82
		0.001	0.24	0.05	0.13	2.32	0.20
1125	0.668	3.391	2.07	55.87	4.62	2658.8	6.55
		0.007	0.02	0.24	0.18	29.1	1.45
1250	2.218	3.337	0.57	53.98	10.50	9713.5	35.84
		0.005	0.01	0.19	0.21	103.0	3.32
1350	0.545	2.830	0.27	38.33	33.49	20356.2	111.78
		0.014	0.00	0.38	0.51	285.6	7.45
1450	0.050	2.501	1.22	30.21	50.34	4513.6	238.84
		0.128	0.15	2.87	39.73	540.2	283.58
1550	0.006	2.275	1.88	25.47	37.67	2931.9	127.56
		0.330	0.49	6.50	14.32	764.4	50.87

(Continued)

Table A-1. (Continued)

Temp. C	39Ar ccSTP/g × e+8	AGE Gyr ±	K/Ca ×100 ±	40/39 ×1 ±	38/39 ×100 ±	37/39 ×100 ±	36/39 ×1000 ±
Techado		9.9 mg J = 0.03002 ± 0.00010					
400	0.070	3.735	21.83	231.09	338.31	251.97	417.44
		0.107	1.54	15.71	53	17.73	78.32
550	0.571	4.349	29.10	338.31	95.46	188.98	9.68
		0.020	0.46	4.05	1.51	3.01	3.04
625	1.388	4.487	39.16	367.92	24.52	140.46	13.09
		0.008	0.45	1.89	0.38	1.60	2.77
675	1.653	4.433	33.77	356.15	23.05	162.85	16.52
		0.008	0.38	1.71	0.34	1.82	2.91
725	1.323	4.481	32.22	366.67	15.50	170.72	14.32
		0.011	0.39	2.44	0.39	2.07	3.08
800	2.923	4.488	28.17	368.25	13.24	195.23	22.94
		0.005	0.30	1.17	0.21	2.05	2.34
850	2.216	4.495	18.50	369.83	14.00	297.34	39.46
		0.006	0.20	1.42	0.26	3.19	3.34
900	1.322	4.241	5.88	316.87	25.70	935.43	116.66
		0.017	0.09	3.39	0.50	13.71	6.66
975	1.200	4.407	3.56	350.52	27.53	1544.22	136.39
		0.012	0.04	2.57	0.48	19.19	7.17
1075	1.045	4.332	4.51	334.91	35.19	1219.13	170.34
		0.013	0.06	2.61	0.57	15.48	8.23
1175	0.682	4.473	2.07	364.94	83.55	2657.6	612.6
		0.019	0.03	4.20	1.37	40.6	15.9
1300	0.133	4.487	0.61	368.18	242.54	9032.0	2153.0
		0.096	0.04	21.33	17.39	533.0	165.6
1550	0.057	4.794	1.07	442.72	504.00	5151.7	4077.9
		0.411	0.26	108.54	168.81	1274.7	1410.1
Miles		30.3 mg J = 0.03007 ± 0.00011					
400	0.479	1.465	20.32	41.74	67.36	270.73	73.87
		0.010	0.29	0.41	0.96	3.84	5.94
500	0.453	3.315	18.59	176.02	39.84	295.89	59.19
		0.009	0.21	1.00	0.46	3.42	6.12
575	0.506	4.056	19.78	282.27	34.98	277.99	103.79
		0.008	0.22	1.42	0.39	3.13	5.41
650	0.828	4.293	27.15	326.55	24.50	202.55	106.53
		0.006	0.29	1.16	0.28	2.16	3.56
700	0.813	4.396	28.77	347.81	19.30	191.16	100.13
		0.006	0.31	1.29	0.24	2.05	3.58
750	1.485	4.411	24.50	350.83	20.04	224.47	109.30
		0.004	0.25	0.86	0.18	2.31	2.07
775	1.500	4.411	22.17	350.82	20.56	248.04	117.19
		0.004	0.23	0.83	0.18	2.55	2.09
800	1.424	4.404	20.50	349.37	21.64	268.26	123.55
		0.003	0.21	0.72	0.18	2.74	2.14
850	1.876	4.414	18.19	351.53	24.98	302.35	141.97
		0.002	0.18	0.51	0.16	3.06	1.69
900	1.377	4.385	14.35	345.35	32.20	383.21	178.54
		0.004	0.15	0.86	0.21	3.95	2.43
950	0.673	4.313	8.69	330.54	49.16	633.15	275.34
		0.008	0.10	1.59	0.40	7.03	4.88
1050	0.909	4.247	2.95	317.67	122.40	1862	732
		0.006	0.03	1.24	0.65	20	5
1150	1.824	4.297	1.70	327.41	167.40	3237	1033
		0.006	0.02	1.19	0.69	34	5
1200	0.559	4.313	0.74	330.83	372.52	7399	2367
		0.010	0.01	1.95	2.65	86	18
1300	0.205	3.763	0.12	235.88	1839.8	44039	12168
		0.039	0.00	5.91	52.7	1184	348
1450	0.023	2.938	0.28	136.69	833.4	19322	6261
		0.134	0.03	12.65	99.6	1861	753
1550	0.019	2.660	28.8	112.27	38.5	191	606
		0.401	8.4	32.35	16.6	56	268

(Continued)

Table A-1. (Continued)

Temp. C	39Ar ccSTP/g × e+8	AGE Gyr ±	K/Ca ×100 ±	40/39 ×1 ±	38/39 ×100 ±	37/39 ×100 ±	36/39 ×1000 ±
Colomera Feldspar		0.81 mg J = 0.05403 ± 0.00020					
400	4.2	4.451	65.71	199.51	65.08	83.71	566.12
		0.017	0.97	2.11	1.09	1.23	13.65
500	6.3	3.194	5.41	90.11	14.13	1017.38	205.14
		0.025	0.11	1.53	0.58	20.02	13.28
550	14.4	3.499	16.39	110.16	3.29	335.51	20.42
		0.013	0.21	0.90	0.21	4.33	3.43
600	27.4	3.852	35.70	137.92	1.91	154.08	9.28
		0.007	0.39	0.62	0.16	1.69	1.35
625	28.3	4.021	81.53	153.32	1.84	67.46	8.41
		0.006	0.87	0.57	0.15	0.72	1.28
650	35.5	4.110	338.52	161.98	1.88	16.25	7.38
		0.004	3.52	0.42	0.14	0.17	1.05
675	95.5	4.142	400.85	165.17	2.15	13.72	8.17
		0.002	4.06	0.21	0.13	0.14	0.54
705	336.7	4.323	823.35	184.58	1.60	6.68	7.41
		0.001	8.29	0.13	0.13	0.07	0.21
725	146.5	4.387	527.38	191.94	1.71	10.43	8.00
		0.002	5.32	0.18	0.13	0.11	0.39
750	110.7	4.403	387.74	193.82	1.68	14.18	7.71
		0.002	3.92	0.21	0.13	0.14	1.43
775	149.3	4.437	633.68	197.78	1.66	8.68	8.04
		0.001	6.39	0.15	0.13	0.09	0.38
800	248.0	4.456	760.77	200.10	1.66	7.23	8.27
		0.001	7.67	0.15	0.13	0.07	0.24
815	246.5	4.464	468.51	201.13	1.71	11.74	9.45
		0.001	4.71	0.17	0.13	0.12	0.24
830	247.5	4.465	699.63	201.26	1.66	7.86	8.24
		0.001	7.05	0.16	0.13	0.08	0.84
850	240.6	4.465	763.63	201.25	1.65	7.20	7.85
		0.001	7.69	0.14	0.13	0.07	0.26
870	214.9	4.469	750.73	201.65	1.66	7.33	8.32
		0.002	7.59	0.22	0.13	0.07	0.15
890	188.8	4.473	661.79	202.16	1.66	8.31	8.31
		0.001	6.67	0.16	0.13	0.08	0.31
915	248.5	4.479	554.24	202.96	1.67	9.92	8.05
		0.001	5.57	0.13	0.13	0.10	0.26
940	222.0	4.480	660.01	202.98	1.67	8.33	8.27
		0.002	6.68	0.24	0.13	0.08	0.18
965	162.3	4.473	496.49	202.20	1.68	11.08	8.46
		0.001	5.00	0.18	0.13	0.11	0.19
1000	178.4	4.465	308.10	201.22	1.73	17.85	8.68
		0.001	3.09	0.13	0.13	0.18	0.19
1050	270.0	4.468	555.29	201.61	1.68	9.90	8.19
		0.001	5.58	0.15	0.13	0.10	0.15
1100	364.9	4.482	637.67	203.28	1.69	8.63	8.30
		0.001	6.40	0.11	0.13	0.09	0.10
1125	217.5	4.488	586.21	203.96	1.70	9.38	8.37
		0.001	5.90	0.16	0.13	0.09	0.21
1150	242.3	4.499	710.59	205.34	1.70	7.74	7.95
		0.001	7.17	0.18	0.13	0.08	0.14
1175	174.3	4.501	699.32	205.62	1.72	7.86	8.32
		0.002	7.06	0.20	0.13	0.08	0.17
1200	100.3	4.507	399.05	206.42	1.78	13.78	9.15
		0.002	4.03	0.22	0.13	0.14	0.29
1250	119.7	4.510	419.24	206.79	1.74	13.12	8.56
		0.001	4.22	0.18	0.13	0.13	0.23
1300	55.8	4.507	252.64	206.39	1.81	21.77	9.78
		0.001	2.54	0.17	0.13	0.22	0.45
1350	12.7	4.485	61.62	203.70	2.01	89.26	7.86
		0.009	0.71	1.15	0.16	1.03	1.21
1450	10.0	4.552	55.78	212.08	2.97	96.60	44.87
		0.015	0.74	1.86	0.19	1.31	3.38
1550	2.4	5.164	14.10	305.16	12.00	390.17	375.50
		0.052	0.45	9.29	0.70	12.50	25.25

(Continued)

Table A-1. (Continued)

Temp. C	39Ar ccSTP/g × e+8	AGE Gyr ±	K/Ca ×100 ±	40/39 ×1 ±	38/39 ×100 ±	37/39 ×100 ±	36/39 ×1000 ±
Sombrerete		13.2 mg J = 0.07225 ± 0.00020					
350	0.63	4.363	82.25	141.06	2884.5	66.87	194.80
		0.010	0.99	0.85	19.1	0.81	3.40
450	0.97	3.949	74.66	109.32	1677.3	73.67	107.90
		0.007	0.83	0.47	8.2	0.81	2.10
500	0.49	4.261	30.71	132.61	191.25	179.10	206.15
		0.013	0.40	1.07	1.81	2.32	4.69
575	0.89	4.476	17.30	151.09	169.47	317.96	360.32
		0.009	0.20	0.81	1.02	3.62	3.25
625	1.23	4.527	15.96	155.80	94.51	344.64	369.51
		0.007	0.17	0.65	0.48	3.73	2.59
675	1.72	4.551	16.29	158.10	66.76	337.68	303.60
		0.005	0.17	0.46	0.30	3.52	1.84
700	1.84	4.572	17.36	160.07	48.64	316.81	258.09
		0.006	0.18	0.57	0.27	3.36	2.09
725	3.39	4.567	17.27	159.60	45.36	318.48	232.07
		0.003	0.18	0.27	0.18	3.23	0.97
750	5.50	4.559	16.86	158.87	43.45	326.18	216.63
		0.002	0.17	0.16	0.15	3.29	4.48
775	8.65	4.546	16.40	157.60	40.05	335.41	205.86
		0.002	0.16	0.14	0.14	3.37	0.49
800	13.16	4.546	15.69	157.57	34.89	350.64	202.44
		0.001	0.16	0.12	0.13	3.52	0.39
825	15.09	4.544	15.00	157.47	32.60	366.69	200.70
		0.001	0.15	0.07	0.13	3.67	0.42
850	14.95	4.542	14.11	157.24	33.26	389.74	204.71
		0.001	0.14	0.08	0.13	3.90	0.30
875	15.56	4.540	13.16	157.07	36.35	417.95	214.68
		0.001	0.13	0.13	0.13	4.19	0.40
900	13.46	4.544	12.56	157.47	39.16	437.74	226.81
		0.001	0.13	0.13	0.14	4.39	0.34
925	10.22	4.539	11.96	156.95	41.98	459.93	240.66
		0.001	0.12	0.10	0.13	4.61	0.38
950	10.94	4.535	10.88	156.57	46.35	505.31	266.99
		0.001	0.11	0.08	0.13	5.06	0.40
975	7.41	4.533	8.75	156.37	62.51	628.59	352.89
		0.001	0.09	0.11	0.14	6.30	0.80
1000	3.43	4.541	8.78	157.19	64.41	626.39	350.08
		0.002	0.09	0.17	0.17	6.30	0.69
1075	3.33	4.536	10.82	156.70	50.27	508.17	278.05
		0.002	0.11	0.18	0.15	5.11	0.83
1200	1.66	4.540	10.33	157.05	59.37	532.61	306.12
		0.003	0.11	0.31	0.24	5.43	1.55
1350	8.26	4.536	9.71	156.72	51.78	566.57	302.27
		0.001	0.10	0.12	0.14	5.68	0.66
1550	1.75	4.502	6.52	153.50	79.40	843.61	447.88
		0.009	0.07	0.86	0.65	9.66	4.27